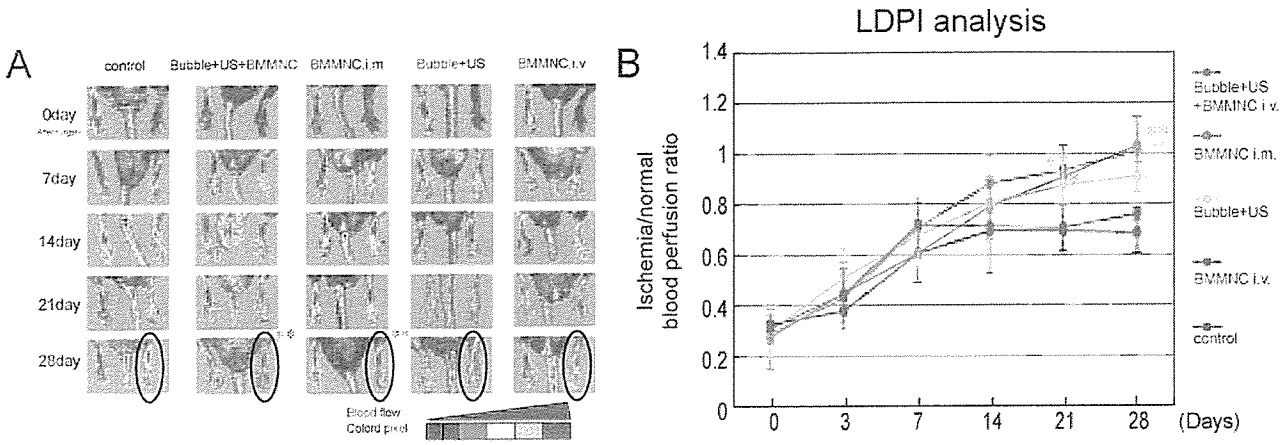

Figure 1. Increase of blood flow by US-microbubble-mediated transfusion of BM-MNCs. A, Representative LDPI. Greater blood perfusion (red to yellow) in ischemic limbs was observed in Bubble+US+BM-MNC infusion, BM-MNC-i.m., and Bubble+US groups in contrast with the untreated control and BM-MNC-i.v. groups. B, Computer-assisted analyses of LDPI revealed a significantly greater blood perfusion in the Bubble+US+BM-MNC-i.v., BM-MNC-i.m., and Bubble+US groups than in the control group. The values shown are mean±SE (n=8) at each time point. *$P<0.05$, **$P<0.01$ vs control.

Laser Doppler Blood Perfusion

Subcutaneous blood perfusion was analyzed by LDPI imaging (Figure 1). Intravenous injection of BM-MNCs (BM-MNC-i.v.) did not cause a significant increase in the blood flow recover compared with the control (saline injection; Figure 1). Treatment with Bubble+US without BM-MNCs-i.v. showed a moderate increase (25±2% at Day 28 versus control, $P<0.05$), whereas the combination of Bubble+US and BM-MNCs-i.v. induced a further increase (34±2% versus control at Day 28, $P<0.01$), which was significantly higher than that of Bubble+US manipulation alone ($P<0.05$). The blood perfusion recovery by Bubble+US+BM-MNC-i.v. was comparable to blood perfusion by BM-MNC-i.m. (38±3%). Blood perfusion after US+BM-MNC-i.v. without Bubble did not significantly differ from those in BM-MNC-i.v. alone or control groups (3±1% versus control at Day 28, n=8; data not shown), suggesting that the combination of BM-MNCs infusion with Bubble+US significantly improves the blood flow recovery after limb ischemia compared with each manipulation alone, and that the efficient cell delivery system depends on US-mediated destruction of microbubbles.

Neocapillary and Arteriole Formation

Formation of capillaries and arterioles was evaluated by factor VIII–positive and SM α-actin–positive vessels. The ratio of capillary/muscle fiber (factor VIII–positive and SM α-actin–negative vessel) was significantly increased in the Bubble+US+BM-MNC-i.v. group (260±15% versus control, $P<0.01$), which was greater ($P<0.01$) than that of Bubble+US group (172±11% versus control, $P<0.05$). The ratio of arteriole/muscle fiber (factor VIII–positive and SM α-actin–positive vessel) was also increased by Bubble+US+BM-MNC-i.v. (188±10% versus control, $P<0.01$), which was greater ($P<0.05$) than that in the Bubble+US group (146±9% versus control, $P<0.05$; Figure 2A). Transfused BM-MNCs (labeled with red fluorescence) were found to be incorporated into microvessels by Bubble+US+BM-MNC-i.v. (arrows in Figure 2B). These findings suggest that Bubble+US+BM-MNC-i.v. enhances both angiogenesis as well as arteriogenesis response.

To examine the specificity of this cell delivery system, we examined the distribution of transfused BM-MNCs in other tissues (kidney, spleen, liver, heart, pancreas, small intestines, and brain) 3 weeks after targeted cell delivery by Bubble+US+BM-MNCs-iv. Small numbers of labeled BM-MNCs were detected in the kidney (mainly in the tubule) and greater numbers of BM-MNCs were observed in the spleen, whereas no labeled cells were detected in other tissues (Figure I, available online at http://atvb.ahajournals.org).

Arteriogenesis Response Evaluated by Angiography

Compared with angiogenesis formed by capillary sprouting, arteriogenesis is often studied with the use of angiography. On the postoperative day 28, all animals were subjected to iliac angiography. Representative angiograms (n=4 in each group) are shown in Figure II (available online at http://atvb.ahajournals.org), in which arrows indicate the ligated ends of femoral arteries. Collateral vessels in the thigh area were quantitatively counted using 5-mm^2 grids.[3,18] An apparent increase in collateral vessel formation was observed in the Bubble+US+BM-MNC-i.v. and BM-MNC-i.m. (4.2±0.2-fold and 4.3±0.2-fold, n=6, respectively; $P<0.001$) compared with that in the BM-MNC-i.v. group. The increase in the Bubble+US group was 1.8±0.1-fold ($P<0.05$) when compared with that in the BM-MNC-i.v. group, which was significantly smaller ($P<0.01$) than that of the Bubble+US+BM-MNC-i.v. group. There was no significant difference between control (saline infusion) and BM-MNC-i.v. groups.

Delivery of Microbubbles to the Ischemic Muscle

Arteriogenesis that restores the regional blood flow was observed 3 days after induction of limb ischemia of rats.[12,13] We therefore performed the infusion of microbubble at day 3 after limb ischemia to efficiently deliver microbubble BR14

Downloaded from atvb.ahajournals.org at SWETS SUBS SERV-#30115043 on March 30, 2007

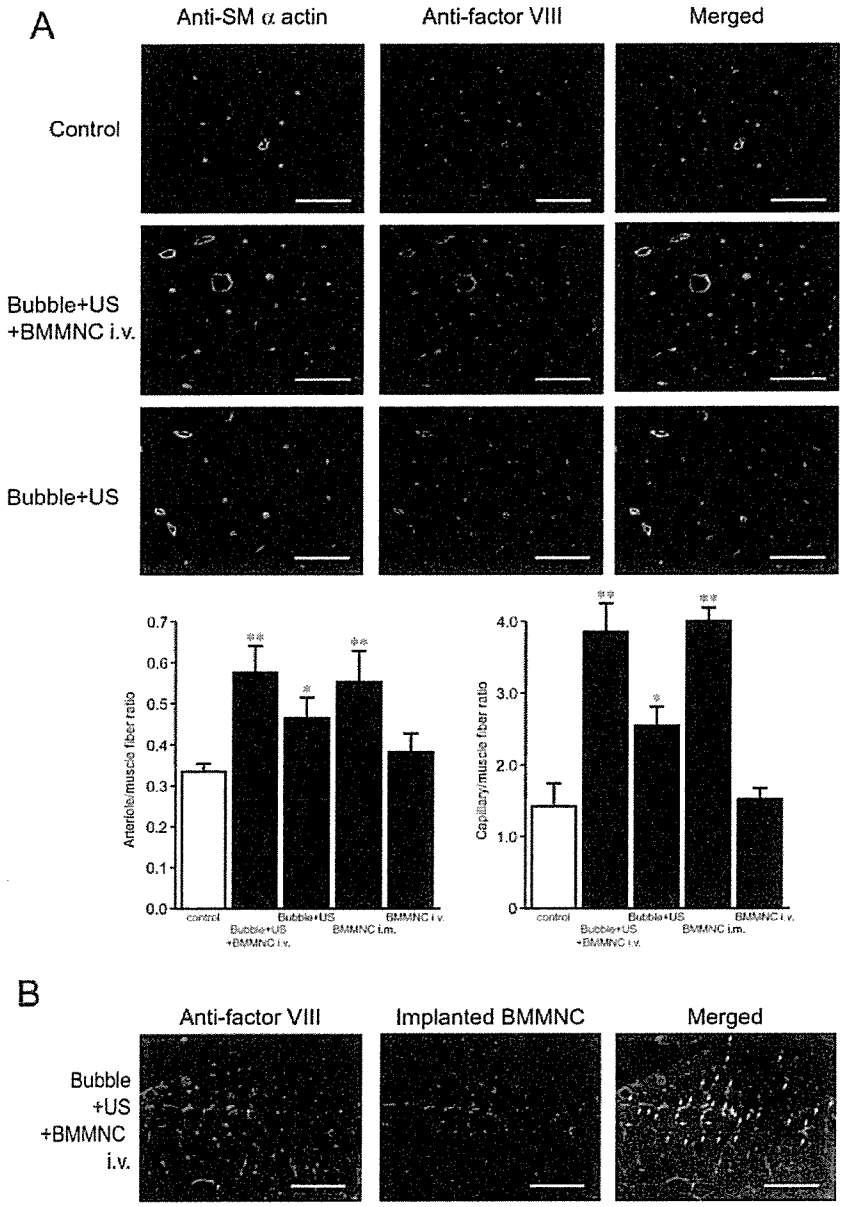

Figure 2. Formation of arterioles/capillaries and incorporation of transfused BM-MNCs. A, Vessels were immunostained with anti-SM α-actin and anti-factor VIII antibodies. Numbers for arterioles (positive for both SM α-actin and factor VIII staining) and capillaries (SM α-actin–negative and factor VIII–positive) were evaluated as a vessel number/muscle fiber ratio (n=8, each group). $^{*}P<0.05$, $^{**}P<0.01$ vs the saline-injected control. Bar=50 μm. B, Incorporation of transfused BM-MNCs (labeled with red-fluorescence). Red-labeled cells were incorporated into factor VIII–positive capillaries (arrows in the merged image) in the Bubble+US+BM-MNC-i.v. group. Data shown are representative of 5 different animals. Bar=200 μm.

to the ischemic site. We further examined whether the transfused microbubbles really reach the hindlimb muscle at 3 days after induction of ischemia. Apparent increase in the contrast densities in the ischemic thigh muscle (indicated by arrows in Figure III, available online at http://atvb.ahajournals.org) was observed ≈15 seconds after injection of microbubbles in both control (normal) and ischemic limbs compared with the pre-images before injection of microbubbles. The increase in contrast shadow diminished after 1 minute of US stimulation, indicating that microbubbles really reach ischemic hindlimb muscles after venous infusion.

Electromicroscopy

A previous study reported the presence of small holes in the endothelial cells treated with Bubble+US,[11] whereas we could not detect the presence of apparent small holes in the vascular endothelium in the skeletal muscle on which the Bubble+US was applied. Neither adhesion of MNCs nor formation of fibrin network including platelets was detected on the surface of normal endothelium or endothelium stimulated by US without microbubbles. Interestingly, we found the attachment of platelets associated with fibrin network and MNCs on the surface of endothelium in all arteries treated by Bubble+US+BM-MNCs infusion (n=6; Figure 3), whereas no adhesion of platelets or MNCs was detected in the US+BM-MNC group without microbubbles (n=6; data not shown).

Induction of Adhesion Molecules

We have reported that transplanted BM-MNCs can firmly attach onto the injured vascular endothelium in an adhesive molecule–dependent manner.[15] We therefore examined the expression profile of adhesive molecules on HUVECs treated by Bubble+US. The expression of adhesive molecules (P-selectin or ICAM-1) was not induced when HUVECs were

Downloaded from atvb.ahajournals.org at SWETS SUBS SERV-#30115043 on March 30, 2007

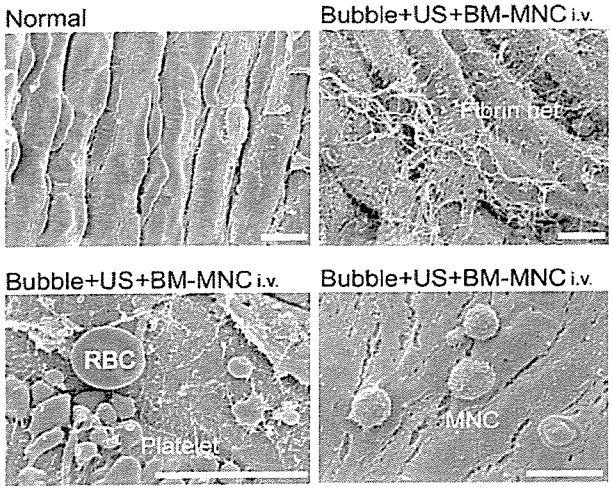

Figure 3. Electron-microscopic appearance of endothelium stimulated by Bubble-US+BM-MNCs. Electron-microscopy showing normal endothelium covered with a monolayer coat (Normal) and appearance of Bubble+US+BM-MNCs i.v.-stimulated endothelium. Attachment of both platelets associated with fibrin network and MNCs was observed on all samples treated by Bubble+US+BM-MNCs i.v. Representative figures are shown (n=4 in each group). Bar=10 μm.

stimulated by Bubble+US in the medium without platelets. Because we found that adhesion of the fibrin network including platelets was consistently observed on the surface of endothelium in all Bubble+US-treated samples (Figure 3), we next examined the involvement of platelet-derived factors in the adhesion of BM-MNCs. Interestingly, the expression of P-selectin (red fluorescence, right panel in Figure 4) and ICAM-1 was markedly induced in both HUVECs and attaching glycoprotein Ib–positive platelets (merged, yellow), when HUVECs were stimulated by Bubble+US in the medium including platelets (only P-selectin data shown in Figure 4).

We also studied whether factors released from the platelets stimulated by Bubble+US are involved in the induction of adhesion molecules. Therefore, we examined the effect of the incubation medium, in which platelet-including medium was stimulated by Bubble+US, on the induction of adhesion molecules. The addition of incubation medium caused the apparent increase in P-selectin expression on HUVECs (red fluorescence, right panel in Figure 4), suggesting that the factors released from the platelets stimulated by Bubble+US are closely involved in the induction of adhesion molecules on HUVECs. Treatment of HUVECs by US alone without microbubbles in the medium including platelets did not induce any expression of adhesive molecules (data not shown). These findings suggest that activation of platelets by Bubble+US and release of platelet-derived proinflammatory factors play a key role in the induction of adhesion molecules in the endothelial cells.

Laminar Flow Assay

We next studied whether the adhesive activity of BM-MNCs on the endothelium was actually modulated by Bubble+US-activated platelets under laminar flow condition. HUVECs were stimulated by Bubble+US in the medium containing platelets and then the adhesion ratio of BM-MNCs on HUVECs was evaluated under laminar flow as previously reported.[15] The presence of platelets in the medium markedly increased the adhesion ratio of BM-MNCs (3.5-fold, $P<0.01$) compared with Bubble+US without platelets (Figure 5). Moderate increase (1.9-fold, $P<0.01$) was observed in the incubation medium group (in which medium including platelets was stimulated by Bubble+US and then added to HUVECs) compared with the ratio in the untreated HUVECs (control). Treatment of HUVECs by US stimulation without microbubbles in the medium including platelets or addition of control medium including platelet alone (without US stimulation) did not cause a significant increase in the adhesion ratio of BM-MNCs compared with the ratio in the untreated HUVEC (data not shown).

Discussion

Angiogenic cell therapy by intramuscular implantation of autologous BM-MNCs was shown to be feasible in patients with ischemic limbs.[2] Because intramuscular implantation is

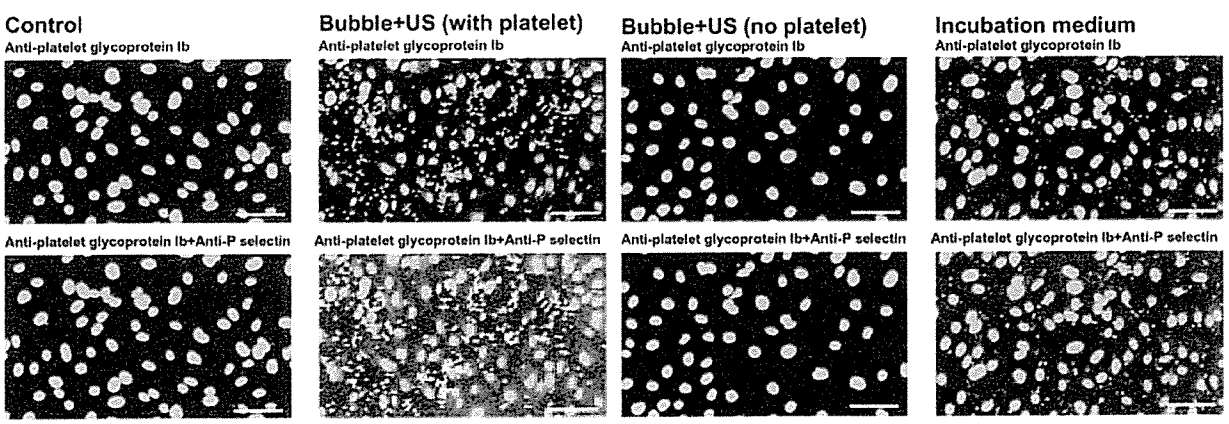

Figure 4. Adhesion of platelets and induction of adhesion molecules on Bubble+US-stimulated HUVECs. The presence of platelets and expression of P-selectin are shown by immunostaining with anti-GP-Ib (green fluorescence) and anti–P-selectin (red fluorescence) antibodies and DAPI staining (blue fluorescence). The expression of P-selectin and adhesion of platelets were observed on HUVECs, when HUVECs were stimulated by Bubble+US in the medium containing 10% platelets or exposed to the incubation medium (in which 10% platelet-including medium was stimulated by Bubble+US). The expression of P-selectin (red fluorescence) on HUVECs and attaching platelets was markedly induced. Bar=50 μm.

Downloaded from atvb.ahajournals.org at SWETS SUBS SERV-#30115043 on March 30, 2007

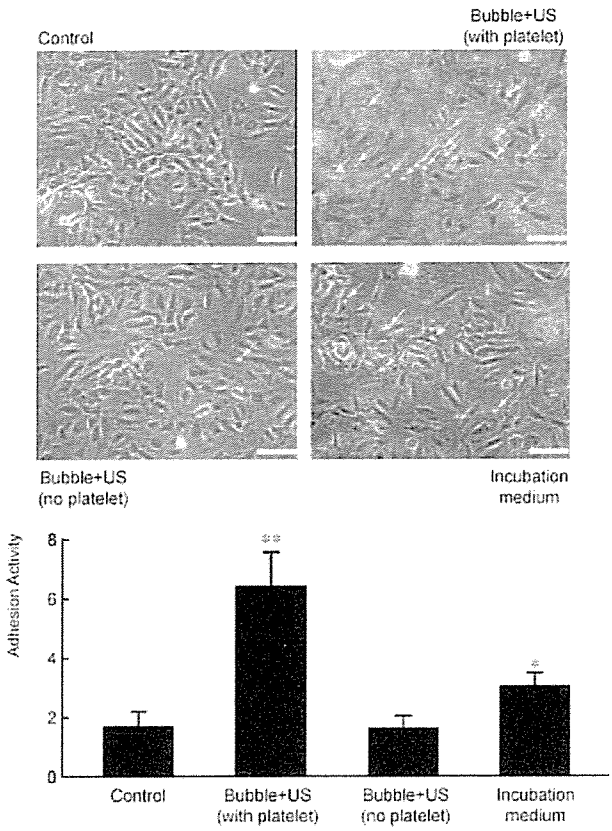

Figure 5. Laminar flow assay of BM-MNCs adhesion. Adhesive activities of BM-MNCs were quantified on HUVEC monolayer under laminar flow. Adhesive cells are indicated by yellow arrows. Cells were considered to be adherent after 10 seconds of stable contact with the monolayer. HUVECs were stimulated by Bubble+US (1MHz, 1.5W, 30 seconds) in the medium with 10% platelets (n=6), without platelets (n=6), or in the incubation medium (in which 10% platelet-including medium was stimulated by Bubble+US, n=6). $^{*}P<0.05$, $^{**}P<0.01$ vs the untreated control. Bar=100 μm.

invasive at the injected sites, the development of a noninvasive cell delivery system that can target vascular endothelium would be a great advantage for the manipulation of angiogenic cell therapy. A new delivery system of drugs or genes has been developed using US-targeted microbubble destruction; the drugs or genes that attach onto gas-filled microbubbles circulate through the intravascular space and are mechanically destroyed within the target organ by ultrasound,[5–11] whereas no studies were reported to determine whether this method is feasible for delivering the "cells" to specific vascular sites.

US-targeted microbubble destruction was reported to cause an inflammatory action on the cell surface by making small holes that revert to a normal appearance within 24 hours.[10,11] Song et al have reported that US-targeted microbubble destruction causes capillary rupturing that stimulates arteriogenesis and an increase in blood flow in both normal[12] and ischemic[13] skeletal muscles, in which angiogenesis response is transient and unlikely contributes to chronic restoration of blood flow. They concluded that arteriogenesis response rather than angiogenesis plays a major role in US+microbubble-stimulated blood flow recovery. We previously demonstrated that the recruitment of BM-MNCs and platelets stimulates angiogenesis response in the ischemic muscles by releasing potent angiogenic factors, such as VEGF or bFGF, and supply of endothelial progenitors.[3,14] Furthermore, we have recently reported that systemically transplanted BM-MNCs can be firmly attached onto the injured vascular endothelium in an adhesive molecule–dependent manner.[15] We therefore expanded the previous studies by Song et al[12,13] and examined whether US-targeted microbubble destruction combined with intravenous transplantation of BM-MNCs causes both angiogenesis and arteriogenesis response in an ischemic hindlimb model, leading to a greater enhancement of blood flow restoration.

We found that (1) intravenous infusion of BM-MNCs combined with US-mediated destruction of microbubbles markedly enhances the restoration of regional blood perfusion in ischemic hindlimbs by stimulating both chronic angiogenesis and arteriogenesis response, and (2) release of platelet-derived proinflammatory factors activated by US-mediated destruction of microbubbles causes the adhesion of transfused BM-MNCs on endothelium by inducing the expression of adhesion molecules (P-selectin and ICAM-1). We found that BM-MNCs transfused intravenously were trapped by the spleen and a few BM-MNCs were present in the renal tubules. Considering that BM-derived hematopoietic stem cells were reported to transdifferentiate to renal tubular cells and improve renal function in the ischemia-reperfusion injury model,[19] the present study establishes for the first time that targeted delivery of BM-MNCs by US destruction of microbubbles is an efficient cell delivery system for therapeutic angiogenesis and arteriogenesis, and that the presence of platelets and/or platelet-derived proinflammatory factors activated by US+microbubbles play an important role in the targeted adhesion of BM-MNCs on vascular endothelium.

Previous studies have indicated that platelet attachment to an inter- or sub-endothelial matrix of endothelial cells promotes selectin-mediated leukocyte adhesion to the damaged endothelium under the flow assay condition.[20,21] Inhibition of P-selectin caused a marked inhibition of leukocyte adhesion at a high shear stress.[20] P-selectin is a receptor for leukocytes and monocytes when its expression is induced on activated platelets and endothelium. This property facilitates rapid adhesion of leukocytes to endothelium in injury tissue regions and enhances platelet-leukocyte interactions at sites of inflammation. Endothelial P-selectin is located on membranes of Weibel-Plade bodies, the secretory granules of endothelium in which large multimers of von Willebrand factor (vWF) are stored.[22] After cellular stimulation with agonists such as thrombin or histamine, P-selectin is rapidly expressed on the endothelial cell surface, making it an excellent candidate for directing adherence of unstimulated leukocytes toward endothelium within minutes of tissue injury.[23] Furthermore, we have reported that BM-MNCs have a higher rolling and adhesive activities because of the greater expressions of adhesive molecules such as P-selectin compared with peripheral blood-derived leukocytes.[15] In this study, we found that factors released from platelets stimulated by microbubble destruction are responsible for the attachment of platelets and BM-MNCs onto the endothelium and the induction of endothelial P-selectin and ICAM-1. The present data from the flow assay also confirm that platelet-derived factors play a key role for adhesion of BM-MNCs onto the endothelial cells under

Downloaded from atvb.ahajournals.org at SWETS SUBS SERV-#30115043 on March 30, 2007

laminar flow. Although we previously showed that platelet-derived VEGF is mainly associated with the angiogenesis response by platelet implantation,[3] preincubation with antibodies for VEGF, bFGF, or PDGF-BB showed no influence on the induction of endothelial P-selectin and ICAM-1 (unpublished observation). Further studies will be required to identify the platelet-derived proinflammatory cytokines responsible for induction of endothelial adhesion molecules. Taken together, these findings suggest that release of platelet-derived proinflammatory factors and direct interaction of platelet onto the endothelial matrix, initiated by US-microbubble destruction, is an underlying mechanism for adhesion of the transfused BM-MNCs on the endothelium under shear stress.

The previous studies showed that US-mediated destruction of microbubbles induces arteriogenesis response in the skeletal muscle, whereas angiogenesis response is transient and unlikely contributes to the increase in the regional blood flow.[12] The arteriogenesis response consists of the formation of new arterioles, which presumably occurs when preexisting capillaries acquire SM coating, and an increase in the diameter of these newly formed and/or preexisting arterioles into channels with larger diameters.[13] Compared with angiogenesis formed by capillary sprouting, arteriogenesis is often studied with the use of conventional angiography. Our angiography finding is consistent with the arteriogenesis response, and the immunohistological data suggest the angiogenesis and arteriogenesis response as evaluated by the increases in capillary numbers and SM coated arterioles, respectively. The neocapillary formation was observed in the day 28 samples, suggesting that the angiogenesis is a chronic response in our study. The controversy with the studies by Song et al[12,13] may be attributable to the difference in the used microbubbles (albumin-coated Optison versus phospholipids-coated BR14). Recruitment of monocytes triggered by monocyte chemoattractant protein-1 was shown to induce arteriogenesis in inflammatory ischemic sites.[24] Because BM-MNCs contain monocyte-lineage progenitor cells,[15] it is plausible that recruitment of BM-MNCs contributes to arteriogenesis together with inflammation response by US+microbubble-mediated capillary rupturing.

In conclusion, the present study demonstrates that intravenous transfusion of BM-MNCs combined with US-destruction of microbubbles is an efficient targeted cell delivery system for therapeutic angiogenesis as well as arteriogenesis, in which the release of platelet-derived proinflammatory factors activated by Bubble+US plays a key role in the attachment of transplanted BM-MNCs onto the endothelial layer.

Acknowledgments

This study was supported in part by research grants from the Ministry of Education, Science, Sports, and Culture, Japan, the Study Group of Molecular Cardiology, the Japan Medical Association, Japan Smoking Foundation, and the Japan Heart Foundation.

References

1. Isner JM, Vale PR, Symes JF, Losordo DW. Assessment of risks associated with cardiovascular gene therapy in human subjects. *Circ Res.* 2001;89:389–400.
2. Tateishi-Yuyama E, Matsubara H, Murohara T, Ikeda U, Shintani S, Masaki H, Amano K, Kishimoto Y, Yoshimoto K, Akashi H, Shimada K, Iwasaka T. Therapeutic angiogenesis for patients with limb ischemia by autologous transplantation of bone-marrow cells: a pilot study and randomized controlled trial. *Lancet.* 2002;360:427–435.
3. Iba O, Matsubara H, Nozawa Y, Fujiyama S, Amano K, Mori Y, Kojima H, Iwasaka T. Angiogenesis by implantation of peripheral blood mononuclear cells and platelets into ischemic limbs. *Circulation.* 2002;106:2019–2025.
4. Shintani S, Murohara T, Ikeda H, Ueno T, Sasaki K, Duan J, Imaizumi T. Augmentation of postnatal neovascularization with autologous bone marrow transplantation. *Circulation.* 2001;103:897–903.
5. Bekeredjian R, Chen S, Frenkel PA, Grayburn PA, Shohet RV. Ultrasound-targeted microbubble destruction can repeatedly direct highly specific plasmid expression to the heart. *Circulation.* 2003;108:1022–1026.
6. Price RJ, Skyba DM, Kaul S, Skalak TC. Delivery of colloidal particles and red blood cells to tissue through microvessel ruptures created by targeted microbubble destruction with ultrasound. *Circulation.* 1998;98:1264–1267.
7. Lawrie A, Brisken AF, Francis SE, Tayler DI, Chamberlain J, Crossman DC, Cumberland DC, Newman CM. Ultrasound enhances reporter gene expression after transfection of vascular cells in vitro. *Circulation.* 1999;99:2617–2620.
8. Shohet RV, Chen S, Zhou YT, Wang Z, Meidell RS, Unger RH, Grayburn PA. Echocardiographic destruction of albumin microbubbles directs gene delivery to the myocardium. *Circulation.* 2000;101:2554–2556.
9. Lindner JR, Kaul S. Delivery of drugs with ultrasound. *Echocardiography.* 2001;18:329–337.
10. Teupe C, Richter S, Fisslthaler B, Randriamboavonjy V, Ihling C, Fleming I, Busse R, Zeiher AM, Dimmeler S. Vascular gene transfer of phosphomimetic endothelial nitric oxide synthase (S1177D) using ultrasound-enhanced destruction of plasmid-local microbubbles improves vasoreactivity. *Circulation.* 2002;105:1104–1109.
11. Taniyama Y, Tachibana K, Hiraoka K, Namba T, Yamasaki K, Hashiya N, Aoki M, Ogihara T, Kaneda Y, Morishita R. Local delivery of plasmid DNA into rat carotid artery using ultrasound. *Circulation.* 2002;105:1233–1239.
12. Song J, Qi M, Kaul S, Price RJ. Stimulation of arteriogenesis in skeletal muscle by microbubble destruction with ultrasound. *Circulation.* 2002; 106:1550–1555.
13. Song J, Cottler PS, Klibanov AL, Kaul S, Price RJ. Microvascular remodeling and accelerated hyperemia blood flow restoration in arterially occluded skeletal muscle exposed to ultrasonic microbubble destruction. *Am J Physiol.* 2004;287:H2754–H2761.
14. Kamihata H, Matsubara H, Nishiue T, Fujiyama S, Tsutsumi Y, Ozono R, Masaki H, Mori Y, Iba O, Tateishi E, Kosaki A, Shintani S, Murohara T, Imaizumi T, Iwasaka T. Implantation of autologous bone marrow mononuclear cells into ischemic myocardium enhances collateral perfusion and regional function via side-supply of angioblasts, angiogenic ligands and cytokines. *Circulation.* 2001;104:1046–1052.
15. Fujiyama S, Amano K, Uehira K, Yoshida M, Nishiwaki Y, Nozawa Y, Jin D, Takai S, Miyazaki M, Egashira K, Imada T, Iwasaka T. Bone marrow monocyte lineage cells adhere on injured endothelium in a monocyte chemoattractant protein-1-dependent manner and accelerate reendothelialization as endothelial progenitor cells *Circ Res.* 2003;93:980–989.
16. Fisher NG, Christiansen JP, Leong-Poi H, Jayaweera AR, Linder JR, Kaul S. Myocardial and microcirculatory kinetics of BR14, a novel third-generation intravenous ultrasound contrast agent. *J Am Coll Cardiol.* 2002;39:530–537.
17. Fisher NG, Leong-Poi H, Sakuma T, Rim SJ, Bin JP, Kaul S. Detection of coronary stenosis and myocardial viability using a single intravenous bolus injection of BR14. *J Am Coll Cardiol.* 2002;39:523–529.
18. Amano K, Matsubara H, Iba O, Okigaki M, Fujiyama S, Imada T, Kojima H, Nozawa Y, Kawashima S, Yokoyama M, Iwasaka T. Enhancement of ischemia-induced angiogenesis by eNOS overexpression. *Hypertension.* 2003;41:156–162.
19. Lin F, Cordes K, Li L, Hood L, Couser WG, Shankland SJ, Igarashi P. Hematopoietic stem cells contribute to the regeneration of renal tubules after renal ischemia-reperfusion injury in mice. *J Am Soc Nephrol.* 2003;14:1188–1199.
20. Kuijper PH, Torres HG, Linden JA, Lammers JW, Sixma JJ, Koenderman L, Zwaginga JJ. Platelet-dependent primary hemostasis promotes selectin-an integrin-mediated neutrophil adhesion to damaged endothelium under flow conditions. *Blood.* 1996:87:3271–3281.
21. Theilmeier G, Lenaerts T, Remacle C, Collen D, Vermylen J, Hoylaerts MF. Circulating activated platelets assist THP-1 monocytoid/endothelial cell interaction under shear stress. *Blood.* 1999;94:2725–2734.
22. McEver RP, Beckstead JH, Moore KL, Marshall-Carlson L, Bainton DF. GMP-140, a platelet alpha-granule membrane protein, is also synthesized by vascular endothelial cells and is localized in Weibel-Palade bodies. *J Clin Invest.* 1989;84:92–99.
23. McEver RP. GMP-140: a receptor for neutrophils and monocytes on activated platelets and endothelium. *J Cell Biochem.* 1991;45:156–161.
24. Heil M, Schaper W. Influence of mechanical, cellular, and molecular factors on collateral artery growth (arteriogenesis). *Circ Res.* 2004;95:449–458.

Downloaded from atvb.ahajournals.org at SWETS SUBS SERV-#30115043 on March 30, 2007

Carbon Dioxide–Rich Water Bathing Enhances Collateral Blood Flow in Ischemic Hindlimb via Mobilization of Endothelial Progenitor Cells and Activation of NO-cGMP System

Hidekazu Irie, MD; Tetsuya Tatsumi, MD, PhD; Mitsutaka Takamiya, MD; Kan Zen, MD; Tomosaburo Takahashi, MD, PhD; Akihiro Azuma, MD, PhD; Kento Tateishi, MD; Tetsuya Nomura, MD; Hironori Hayashi, MD; Norio Nakajima, MD; Mitsuhiko Okigaki, MD, PhD; Hiroaki Matsubara, MD, PhD

Background—Carbon dioxide–rich water bathing has the effect of vasodilatation, whereas it remains undetermined whether this therapy exerts an angiogenic action associated with new vessel formation.

Methods and Results—Unilateral hindlimb ischemia was induced by resecting the femoral arteries of C57BL/J mice. Lower limbs were immersed in CO_2-enriched water (CO_2 concentration, 1000 to 1200 mg/L) or freshwater (control) at 37°C for 10 minutes once a day. Laser Doppler imaging revealed increased blood perfusion in ischemic limbs of CO_2 bathing (38% increase at day 28, $P<0.001$), whereas N^G-nitro-L-arginine methyl ester treatment abolished this effect. Angiography or immunohistochemistry revealed that collateral vessel formation and capillary densities were increased (4.1-fold and 3.7-fold, $P<0.001$, respectively). Plasma vascular endothelial growth factor (VEGF) levels were elevated at day 14 (18%, $P<0.05$). VEGF mRNA levels, phosphorylation of NO synthase, and cGMP accumulation in the CO_2-bathed hindlimb muscles were increased (2.7-fold, 2.4-fold, and 3.4-fold, respectively) but not in forelimb muscles. The number of circulating Lin−/Flk-1+/CD34− endothelial-lineage progenitor cells was markedly increased by CO_2 bathing (24-fold at day 14, $P<0.001$). The Lin−/Flk-1+/CD34− cells express other endothelial antigens (endoglin and VE-cadherin) and incorporated acetylated LDL.

Conclusions—Our present study demonstrates that CO_2 bathing of ischemic hindlimb causes the induction of local VEGF synthesis, resulting in an NO-dependent neocapillary formation associated with mobilization of endothelial progenitor cells. (***Circulation.* 2005;111:1523-1529.**)

Key Words: carbon dioxide ■ hypercapnia ■ angiogenesis ■ stem cells ■ endothelium ■ vasculogenesis

Carbon dioxide–rich (CO_2) water bathing has a long history and is thought to be effective in the treatment of peripheral vascular disorder[1]; however, the mechanism(s) underlying this traditional therapy remains poorly defined. The effect of CO_2-enriched water on cutaneous circulation depends primarily on the vasodilatation elicited by the CO_2 that diffuses into the subcutaneous tissue through the skin layers.[2,3] Findings in the intact coronary circulation[4] and in isolated aortic strips[5] have suggested that vasodilation in response to CO_2 may be mediated in part by nitric oxide (NO).

Previous investigations have provided inferential evidence that biological processes modulated by NO might extend to include angiogenesis. Direct in vitro evidence that NO may induce angiogenesis was demonstrated recently by Papapetropoulos et al.[6,7] Ziche et al[8,9] established the first line of evidence that NO can induce angiogenesis in vitro. Murohara et al[10] clearly showed NO-mediated angiogenesis in response to tissue ischemia in NO-deficient mice. We have also reported that overexpression of endothelial NO synthase (eNOS) causes a marked increase in neocapillary formation in response to tissue ischemia.[11] Furthermore, hypercapnia-associated acidosis was reported to induce the expression of angiogenic factors, vascular endothelial growth factor (VEGF), or basic fibroblast growth factor and inhibit endothelial cell apoptosis.[12] Taken together, this accumulated evidence may raise the possibility that the CO_2-enriched water bathing therapy enhances regional blood perfusion by increasing new vessel formation. In the present study, we report that CO_2-enriched water bathing stimulates blood flow restoration in the ischemic hindlimbs of mice by increasing NO-dependent collateral vessel formation and the mobilization of endothelial-lineage progenitor cells into the circulation.

Methods

Principle of the Device

This device uses a CO_2 gas–permeable membrane similar to the principle of an artificial lung on the extracorporeal circulatory system. The unit consists of 15 000 multilayered composite-membrane hollow fibers with porous membrane sandwiching on

Received June 1, 2004; revision received November 13, 2004; accepted November 19, 2004.

From the Department of Cardiovascular Medicine, Kyoto Prefectural University School of Medicine, Kyoto, Japan.

Correspondence to Hiroaki Matsubara, MD, Department of Cardiovascular Medicine, Kyoto Prefectural University of Medicine, Kamigyo-Ku, Kyoto, 602-8566, Japan. E-mail matsubah@koto.kpu-m.ac.jp

© 2005 American Heart Association, Inc.

Circulation is available at http://www.circulationaha.org

DOI: 10.1161/01.CIR.0000159329.40098.66

both sides of gas-permeable membrane (Mitsubishi-Leiyon) and is capable of instantly converting 20 L/min of water (pH 7.0) into CO_2-enriched water (free CO_2 concentration, 1000 to 1200 mg/L, pH 5.0).

Mouse Model of Unilateral Hindlimb Ischemia and CO_2 Bathing

Unilateral hindlimb ischemia was induced by resecting the right femoral arteries (including muscle branches) and veins of 8-week-old male C57BL/J mice under anesthesia with sodium pentobarbital (50 mg/kg IP).[11,13] To inhibit NOS chronically, the mice were provided water containing 1 mg/mL N^G-nitro-L-arginine methyl ester (L-NAME) for 4 weeks.[11] Because CO_2 bathing immediately after operation delayed the closure of this skin wound, we started the CO_2 bathing of the lower limb from 4 days after surgery. Lower limbs of mice were immersed into CO_2-enriched water for 10 minutes or freshwater (control) at 37°C once a day under anesthesia (n=10 in each group). The Institutional Animal Care and Use Committee of our university approved all animal protocols.

Immunohistochemistry

Four pieces of ischemic tissues from the adductor and semimembranous muscles were obtained 28 days after the surgery of hindlimb ischemia. Frozen sections were stained with anti-factor VIII, followed by incubation with TRIC-conjugated secondary antibody. Five fields from 2 muscle samples of each animal were randomly selected for capillary counts. To ensure that capillary densities were not overestimated as a consequence of myocyte atrophy or underestimated because of interstitial edema, the capillary/muscle fiber ratio was determined.[11,13] To examine whether cells survived in the tissues, adjacent sections were subjected to alkaline phosphatase staining by the indoxyl-tetrazolium method. Alkaline phosphatase staining turns capillary endothelial cells a dark blue color only when they are viable and when the intracellular enzyme activity remains intact.[11,13]

Laser Doppler Analysis and Angiography

We measured the ratio of the ischemic (right)/normal (left) limb blood flow by use of a laser Doppler perfusion image (LDPI) analyzer (Moor Instruments). After blood flow had been scanned twice, stored images were subjected to computer-assisted quantification of blood flow, and average flows of the ischemic and nonischemic limbs were calculated. To minimize data variables caused by ambient light and temperature, the LDPI index was expressed as the ratio of ischemic (left) to nonischemic (right) limb blood flow.[11,13]

Vessel density was evaluated with a microfocus x-ray television device (Hitex Co Ltd) 28 days after ischemia (n=5). Longitudinal laparotomy was performed to introduce a catheter into the abdominal aorta, followed by injection of contrast medium (lipiodol). Angiography was performed for 2 seconds after the injection. We quantitatively analyzed collateral vessel numbers as previously reported.[11,13] Briefly, numbers of vessels in the thigh area were counted by use of 5-mm^2 grids by 2 radiologists who were unaware of the group identity of the angiographic film. Interobserver variation was <5%.

cGMP Assay and Measurement of Blood pH Level

The assay for tissue cGMP was performed by use of the cGMP enzyme immunoassay system (Biotrak; Amersham) as previously described.[11] The tissues remaining after cGMP measurement were digested by use of a bicinchoninic acid protein assay kit (Pierce). Blood pH levels were measured by automated blood gas analyzer (ABL505, Radiometer A/S).

Northern and Western Blotting and Plasma VEGF Measurement

Frozen skeletal samples from hindlimbs or forelimbs were homogenized in Trizol reagent (Gibco BRL). Blots were hybridized with a random-primed ^{32}P-labeled cDNA probe for VEGF[11] and normalized by densities for GAPDH as an internal control. Hybridized signals were measured by scanning densitometry, and VEGF mRNA levels were arbitrarily normalized relative to the GAPDH mRNA levels.

Phosphorylation of eNOS (serine 1177) was analyzed by Western blotting using phospho-specific antibodies (New England Biolabs). The muscles were homogenized in lysis buffer. Lysates were immunoblotted with anti-phospho antibodies and detected with an enhanced chemiluminescence kit (Amersham).[11] Plasma VEGF concentration was measured by use of the ELISA kit (R&D Systems).

FACS Staining

Total nuclear cells in the peripheral blood were isolated by erythrocyte lysis with ammonium chloride solution (PharM Lyse, Becton Dickinson). Lin−/Flk+ cells were isolated by PE-labeled lineage antigens (CD11b, CD3, B220, Ter-199, Gr-1, CD4, CD8e, CD16/32), FITC-CD34, and biotin-Flk-1 and then analyzed by use of a FACScan flow cytometer.[14,15] Lin−/Flk+/endoglin+ cells were isolated by FITC-labeled lineage antigens, PE–Flk-1 and biotin-endoglin. To prove the specificity of anti-CD34 antibody, the biotin-labeled anti-mouse CD34 antibody used in this study was reacted with mouse bone marrow cells and purified with streptavidin-magnet beads, followed by fluorescence-activated cell sorter (FACS) analysis using streptavidin-PE. All anti-mouse antibodies were purchased from BD Biosciences.

Differentiation of Lin−/Flk-1+ Cells Into Endothelial Cells In Vitro

The population of Lin−/Flk-1+ cells was isolated with FACS from the peripheral blood of the mice that had undergone the limb ischemic operation and then treated with CO_2 bathing for 14 days. These cells were cultured on fibronectin-coated plastic dishes in DMEM supplemented with 100 ng/mL VEGF and 10% FBS. After 4 days, DiI-labeled acetylated LDL (Biomedical Technologies Inc) was added into medium at 2 μg/mL for 6 hours, fixed with 4% paraformaldehyde, and stained with anti–VE-cadherin antibody and FITC-labeled anti-IgG antibody.

Statistics

Statistical analyses were performed by 1-way ANOVA followed by pairwise contrasts using Dunnett's test. Data (mean±SEM) were considered significant at a value of $P<0.05$.

Results

Laser Doppler Blood Perfusion

Progressive recovery of limb perfusion was disclosed in CO_2-bathed and control freshwater-bathed mice after induction of limb ischemia. A greater degree of blood perfusion recovery was observed in the ischemic limbs of CO_2-bathed mice compared with controls (38% increase at day 28, $P<0.001$) (Figure 1, A and B). Inhibition of NOS activity by L-NAME administration abolished an enhancement of blood flow recovery by CO_2 bathing and reversed the recovery ratio toward the control level. Blood flow in L-NAME–treated mice tended to be lower than that in wild-type mice, but this difference was not significant (Figure 1B).

Angiography

All animals were subjected to iliac angiography using contrast medium (lipiodol) on postoperative day 28. Collateral vessel numbers were markedly increased in ischemic limbs of CO_2-bathed mice (4.1±0.4-fold at day 28, $P<0.001$, n=5) compared with those in water-bathed mice (Figure 2).

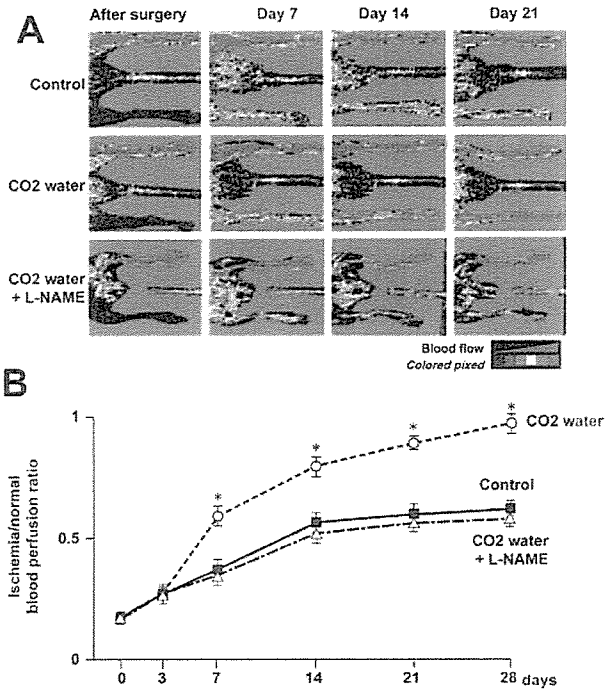

Figure 1. LDPI. A, Greater blood perfusion (red to yellow) was observed in CO_2-enriched water-bathed limbs, in contrast to reduced perfusion (green to blue) in freshwater-bathed ischemic limbs (control). B, Computer-assisted analyses of LDPI revealed significantly greater blood perfusion values in CO_2-enriched water-bathed group than in control group. Administration of L-NAME (1 mg/mL) in drinking water reduced increased perfusion by CO_2-enriched water bathing toward normal level. Values shown are mean±SEM (n=10) at each time point. *P<0.001 vs control mice.

Analysis of Capillary Density

Immunohistochemical staining for anti-factor VIII revealed the presence of capillary endothelial cells (Figure 3A). The capillary/muscle fiber ratio in the skeletal muscle obtained 28 days after hindlimb ischemia was significantly increased in the CO_2-bathed mice (3.7-fold, P<0.001) compared with that in water-bathed mice. A similar increase (4.2-fold increase, P<0.001) was also observed in ALP staining for detection of viable endothelial cells (Figure 3B). Administration of L-NAME (1 mg/mL) in drinking water reduced the increased vessel numbers by CO_2 bathing toward the normal level (Figure 3).

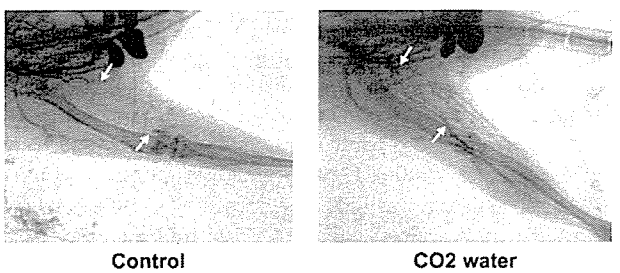

Figure 2. Angiographic analysis. Representative angiograms were obtained on postoperative day 28. Arrows indicate ligated ends of femoral arteries. Collateral vessel numbers counted by use of 5-mm^2 grids were markedly increased in ischemic limbs of CO_2-bathed mice (4.1±0.4-fold at day 28, P<0.001, n=5) compared with those in water-bathed mice.

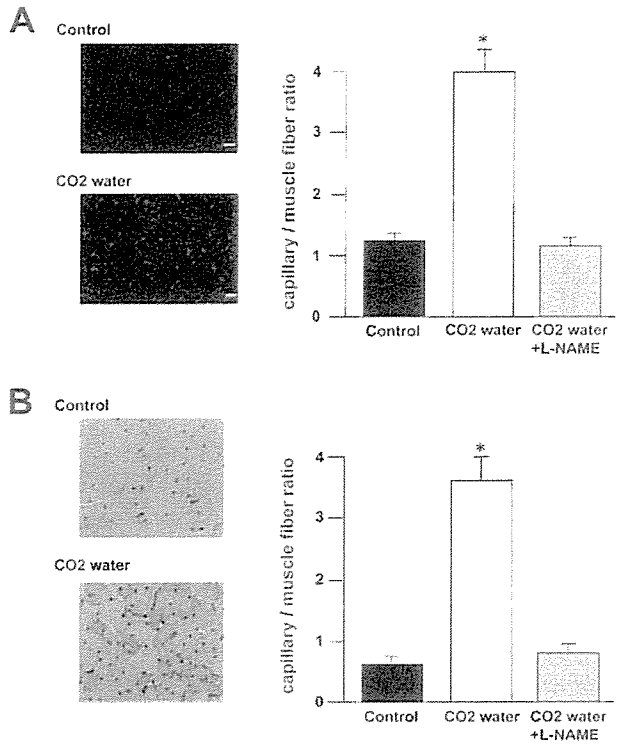

Figure 3. Immunohistochemical analysis. A, Ischemic tissues from adductor and semimembranous muscles were obtained 28 days after surgery of hindlimb ischemia. Endothelial cells were stained with anti-factor VIII antibody, followed by incubation with TRIC-conjugated secondary antisera. B, Alkaline phosphatase staining turns viable endothelial cells blue. Five fields from 2 muscle samples of each animal (n=10) were randomly selected, and capillary density was shown as capillary/muscle fiber ratio. Administration of L-NAME (1 mg/mL) in drinking water reduced increased vessel numbers by CO_2 bathing toward control levels of freshwater-bathed ischemic limbs (n=10). *P<0.001 vs control mice. Bars=50 μm.

Induction of VEGF Expression, eNOS Phosphorylation, and cGMP Levels

VEGF mRNA levels were examined in hindlimb muscles dissected at days 0 (before), 1, 2, 7, 14, and 21. VEGF mRNA levels were decreased immediately after hindlimb ischemia (day 1, day 2), and then gradually reverted to the basal levels at day 7 in the control group. In the CO_2-enriched water group, a marked increase in VEGF mRNA levels was observed at day 7 (1.6-fold versus day 0 preischemic levels, P<0.01) and showed a peak level at ≈day 14 (2.7-fold versus day 0, P<0.001). Induction of the VEGF mRNA from the preischemic level was significantly higher in the CO_2 bathing group than the increase in the control group (Figure 4), whereas the increase in VEGF mRNA synthesis by CO_2 bathing was not affected by L-NAME treatment (Figure 5A).

To define whether the effect of CO_2 bathing results from systemic or local VEGF synthesis, we examined the time-dependent VEGF mRNA induction in forelimb skeletal muscles after CO_2 bathing and changes in plasma VEGF levels. The mRNA levels in forelimb skeletal muscles of CO_2-bathed

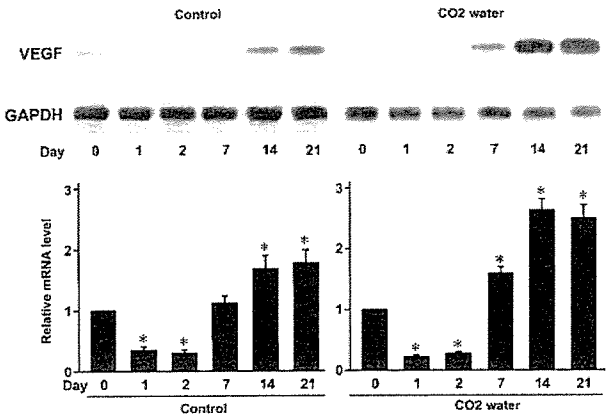

Figure 4. VEGF mRNA expression in ischemic hindlimb. Hindlimb skeletal muscles were dissected after ischemia, and RNA was extracted. Densities of VEGF mRNA signals were measured by densitometry and normalized relative to those of GAPDH mRNA signals. Results (mean±SEM, n=6) were arbitrarily indicated as values relative to VEGF mRNA levels at day 0. *P<0.001 vs day 0 preischemic levels.

ischemic mice did not change significantly after CO_2 bathing compared with the preischemic levels (Figure 5A). Although only induction of hindlimb ischemia did not affect plasma VEGF levels, VEGF levels in the CO_2-bathed ischemic mice were slightly but significantly elevated at day 14 (18%, P<0.05, n=6) compared with the water-immersed ischemic mice (n=6) (Figure 5B). Furthermore, we determined plasma pH levels to study whether CO_2 bathing–mediated effects are systemic. We found that CO_2 bathing of ischemic lower limbs did not significantly affect the pH levels in the peripheral blood (control, 7.2±0.04; CO_2 bathing, 7.2±0.03 at day 14; n=6 each). These findings demonstrate that VEGF synthesis by CO_2 bathing is induced only locally and that this increase in local VEGF synthesis leads to the elevation in plasma VEGF levels.

Skeletal muscles at day 14 (in which VEGF expression is maximally increased) were dissected, and eNOS phosphorylation and cGMP levels were examined. The eNOS phosphorylation levels at day 14 (normalized with expression levels of eNOS protein) were increased significantly in both control and CO_2-enriched water groups relative to the day 0 preischemic levels (1.6- and 2.4-fold, respectively) (Figure 6A). eNOS phosphorylation levels in the CO_2-enriched water group were significantly higher than those in the control group (P<0.001 versus the control group). Consistent with eNOS phosphorylation, cGMP levels in skeletal muscles at day 14 were also significantly higher (3.4-fold, P<0.001) in the CO_2-enriched water group compared with those in the control group (Figure 6B).

Effect of CO_2 Bathing on Circulating Endothelial-Lineage Progenitor Cells

CD34+/AC133+/Flk-1+ hematopoietic stem cells circulate in the peripheral blood of humans as an endothelial precursor cell and play a critical role in neovascularization in ischemic tissue.[16] Because AC133 marker is not available for mice, we isolated hematopoietic lineage-negative (Lin−) cells from the peripheral blood and then analyzed the CD34- and endothelial markers Flk-1– and endoglin-positive population to study whether endothelial-lineage precursor cells are mobilized by CO_2-enriched water bathing. FACS analysis indicated that Lin−/Flk-1+ cells are barely detected in the peripheral blood of normal mice (0.01±0.002% of total nuclear cells, n=12). Lin−/Flk-1+ cells were significantly increased after limb ischemia and showed a peak value at day 14 (≈7-fold versus the preischemic value) (from 0.01±0.002% to 0.073±0.002%, P<0.001, n=7). Interestingly, such a Lin−/Flk-1+ population was further increased by CO_2 bathing and showed a peak value at day 14 (≈24-fold increase, from 0.01±0.002% to 0.24±0.03%, P<0.001, n=7) (Figure 7A). The Lin−/Flk-1+ cells mobilized by CO_2 bathing were mostly positive for anti-endoglin antibody and in the CD34-negative fraction (Figure 7B). Considering that CD34−/Flk-1+ cells rather than CD34+/Flk-1+ are reported to be a real population of hematopoietic stem cells,[17] our present data

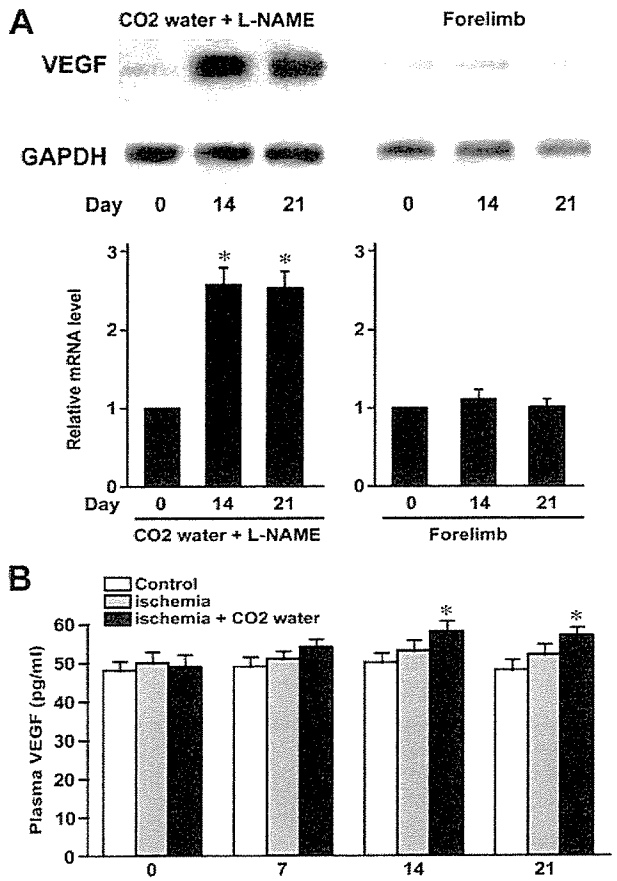

Figure 5. Effect of L-NAME on VEGF mRNA expression in hindlimb and forelimb skeletal muscles after hindlimb ischemia and plasma VEGF concentrations. A, Mice with hindlimb ischemia were provided water containing 1 mg/mL L-NAME, and time-dependent VEGF mRNA expression was measured as described in Figure 4. Forelimb skeletal muscles were dissected from hindlimb ischemia mice, and VEGF mRNA was analyzed. Results (mean±SEM, n=5) were arbitrarily indicated as values relative to VEGF mRNA levels at day 0. *P<0.001 vs day 0 preischemic levels, B, Plasma VEGF concentrations were measured by ELISA (control, CO_2 bathing of normal mice; ischemia, freshwater-bathed ischemic mice; ischemia+CO_2 water, CO_2-bathed ischemic mice, n=5 each). *P<0.05 vs day 0.

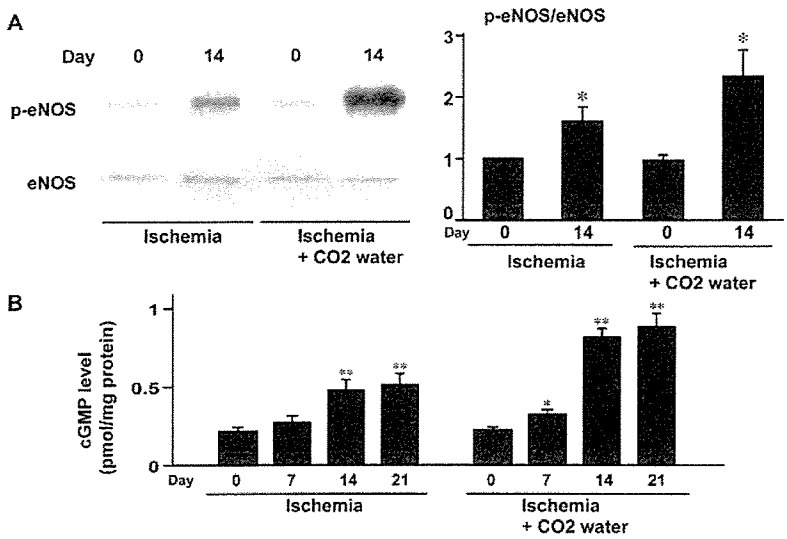

Figure 6. cGMP accumulation in ischemic limbs. A, Skeletal muscles were homogenized and immunoblotted with anti-phospho antibodies for eNOS. Phospho signals in filters were stripped and reprobed with anti-eNOS antibody. Phospho-eNOS densities were measured by densitometry and normalized relative to those of eNOS signals. Results are arbitrarily indicated as values relative to signal densities in day 0 preischemic control. Results shown are mean±SEM (n=6), and representative data are shown. *$P<0.001$ vs values in day 0 preischemic control. B, Skeletal muscles were dissected at days 7, 14, and 21 after hindlimb ischemia, and tissue cGMP levels were measured. Results shown are mean±SEM (n=6 each). *$P<0.05$, **$P<0.001$ vs day 0 preischemic control.

indicate that CO_2-enriched water bathing mobilizes very immature hematopoietic stem cells, including endothelial progenitor cells. To prove the specificity of anti-CD34 antibody, CD34+ cells were enriched by anti-mouse CD34 antibody from mouse bone marrow cells. As shown in Figure 7C, 83% purity of CD34-positive cells was detected by FACS, indicating that the staining for the CD34 antigen was properly performed.

We further examined whether Lin−/Flk-1+ cells express another endothelial marker, VE-cadherin, and also possess the characteristics of endothelial cells, such as acetylated LDL uptake. The Lin−/Flk-1+ cell population, mobilized by CO_2 bathing, was isolated and cultured with 100 nmol/L VEGF-supplemented medium for 4 days. Approximately 26±1.2% (n=12) of the Lin−/Flk-1+ cells adhered onto the fibronectin-coated plastic dishes. Approximately 74±2.3% (n=12) of the attaching cells showed the ability to incorporate the DiI-labeled acetylated LDL, and these cells expressed the VE-cadherin (Figure 7D).

Discussion

A number of reports about the physiological effects of CO_2-enriched water on subcutaneous microcirculation have been published. Savin et al[18] reported that transfer of CO_2 across the skin can have beneficial local vasomotor effects. Hartmann et al[19] demonstrated an increase in tissue oxygen brought about by the Bohr effect in addition to the vasodilation effect by CO_2 or vasodilation by decrease in plasma catecholamine levels. Toriyama et al[20] also reported that the effect of CO_2-enriched water on the subcutaneous microcirculation results from peripheral vasodilation resulting from increased parasympathetic and decreased sympathetic nerve activity. Findings in the intact coronary circulation[4] and in isolated aortic strips[5] have suggested that vasodilation in response to CO_2 may be mediated in part by NO. Consistent with these previous studies, our present study demonstrates that immersion of ischemic hindlimb into CO_2-enriched water bathing causes an NO-dependent increase in collateral blood perfusion, induction of regional VEGF synthesis, and mobilization of endothelial-lineage progenitor cells into the circulation.

What is the mechanism responsible for the proangiogenic effect by CO_2-enriched water bathing? In the endothelial cells cultured in the medium equilibrated with hypercapnia-associated acidosis, the expressions of potent angiogenic factors, such as VEGF or basic fibroblast growth factor, are increased and endothelial cell apoptosis is inhibited.[12] VEGF was well known to mobilize endothelial progenitor cells from bone marrow into the circulation.[21] Our present data clearly indicate that VEGF expression is markedly induced in hindlimb skeletal muscles after CO_2-enriched water bathing. A high concentration of CO_2 (1000 to 1200 mg/L) liberates free CO_2 in the freshwater (pH 7.0), resulting in a decrease in pH level (pH 5.0). We found that CO_2 bathing of ischemic lower limbs did not affect the pH levels in the peripheral blood and VEGF mRNA synthesis in the forelimb muscle. Considering that acidosis induces VEGF expression in the endothelial cells,[12] the local tissue acidosis by CO_2 bathing, rather than the CO_2 content of the water, may induce VEGF synthesis in the local skeletal muscles. Furthermore, calcium mobilization associated with local tissue pH changes may serve as alternate, or contributory, mechanisms for these observations.

Previous studies reported that VEGF stimulates the release of NO from the arterial wall[22,23] and promotes the recovery of disturbed endothelium-dependent flow in the ischemic hindlimb.[24] Involvement of NO in the angiogenic properties of VEGF has been established in the NO-deficient mice; Murohara et al[10] showed NO-mediated angiogenesis in the hindlimb ischemia model, and Aicher et al[25] reported that VEGF-mediated mobilization of endothelial progenitor cells is reduced in NO-deficient mice. The present study revealed that inhibition of NOS activity by L-NAME inhibited the recovery of collateral blood flow by CO_2 bathing without affecting local VEGF synthesis. Taken together, these findings demonstrate that the proangiogenic effect by CO_2 bathing is a result of activation of NO-mediated signaling and that this activation results from the downstream effects of VEGF. Considering that VEGF-mediated mobilization of endothelial

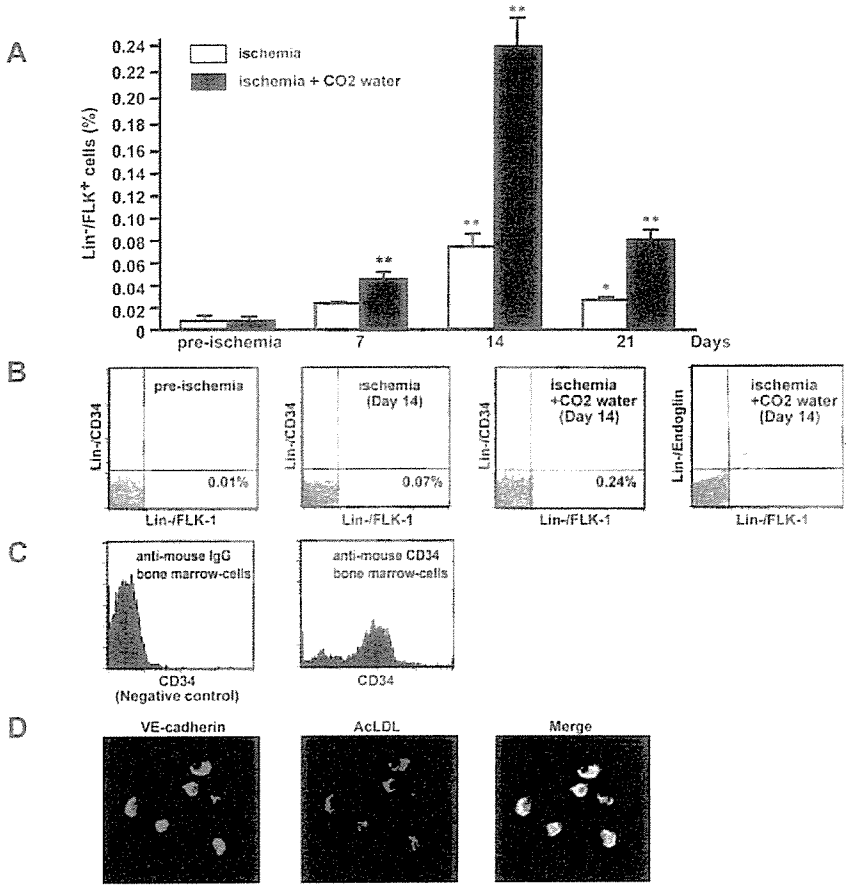

Figure 7. FACS analysis of circulating endothelial-lineage progenitor cells. A and B, Lin−/Flk+ cells in peripheral blood nuclear cells were isolated by PE-labeled lineage antigens, FITC-CD34 and biotin–Flk-1, and then analyzed. Lin−/Flk+/endoglin+ cells were isolated by FITC-labeled lineage antigens, PE-Flk-1 and biotin-endoglin. Cell number ratio of Lin−/Flk+ cells to total nuclear cells is shown (n=6 each). $^*P<0.05$, $^{**}P<0.001$ vs day 0 preischemic control. **C,** To prove specificity of anti-CD34 antibody, CD34+ cells in mouse bone marrow cells were enriched by biotin-labeled anti-mouse CD34 antibody and purified with streptavidin-magnet beads, followed by FACS analysis using streptavidin-PE. Rat anti-mouse IgG was used as a negative control. D, Lin−/Flk+ cells were cultured on fibronectin-coated plastic dishes in DMEM supplemented with 100 ng/mL VEGF and 10% FCS. After 4 days, DiI-labeled acetylated LDL was added into medium at 2 μg/mL for 6 hours, fixed with 4% paraformaldehyde, and stained with anti–VE-cadherin antibody and FITC-labeled anti-IgG antibody.

progenitor cells is NO-dependent,[25] our present study suggests that CO_2 bathing causes the induction of local VEGF synthesis, resulting in an NO-dependent neocapillary formation associated with mobilization of endothelial progenitor cells.

Hartman et al[19] reported that repeated CO_2-enriched water bathing increases arterial flow, transcutaneous oxygen tension, and pain-free walking distance in the clinical trial of peripheral arterial disease. Although they have not performed angiography, the enhancement of neovascularization may cause the increases in walking distance in addition to the improvement of blood vessel function. Toriyama et al[20] also showed that CO_2 foot bathing is clinically effective in the salvage of critical limb ischemia. In conclusion, our present study clearly demonstrates for the first time that CO_2-enriched water bathing causes the enhanced induction of local VEGF synthesis associated with activation of the NO-cGMP pathway and mobilization of endothelial progenitor cells, resulting in NO-dependent neocapillary formation that leads to an increase in collateral blood flow. Thus, these findings indicate that the CO_2-enriched water bathing therapy can be included in angiogenic therapies associated with neovascularization, such as the transplantation of bone marrow mononuclear cells[14] or VEGF gene therapy.[26]

Acknowledgments

This study was supported in part by Grants-in-Aid from the Ministry of Education, Science, and Culture and from the Ministry of Health, Labor, and Welfare, and by the Uehara Memorial Grant in Japan. We thank Yoshimi Togawa for expert assistance in the experiment.

References

1. Blair DA, Glover WE, McArrdle L. The mechanism of the peripheral vasodilation following carbon dioxide inhalation in man. *Clin Sci.* 1960; 19:407–423.
2. Schnizer W, Erdl R, Schops P, Seichert N. The effects of external CO_2 application on human skin microcirculation investigated by laser Doppler flowmetry. *Int J Microcirc Clin Exp.* 1985;4:343–350.
3. Ito T, Moore JI, Koss MC. Topical application of CO_2 increases skin blood flow. *J Invest Dermatol.* 1989;93:259–262.
4. Gurevicius J, Salem MR, Metwally AA, Silver JM, Crystal GJ. Contribution of nitric oxide to coronary vasodilation during hypercapnic acidosis. *Am J Physiol.* 1995;268:H39–H47.
5. Fukuda S, Matsimoto M, Nishimura N, Fujiwara N, Shimoji K, Takeshita H, Lee TJ. Endothelial modulation of norepinephrine-induced constriction of rat aorta at normal and high CO_2 tensions. *Am J Physiol.* 1990;258:H1049–H1054.
6. Papapetropoulos A, Desai KM, Rudic RD, Mayer B, Zhang R, Ruiz-Torres MP, Garcia-Cardena G, Madri JA, Sessa WC. Nitric oxide synthase inhibitors attenuate transforming-growth-factor-β1–stimulated capillary organization in vitro. *Am J Pathol.* 1997;150:1835–1844.
7. Papapetropoulos A, Garcia-Cardena G, Madri JA, Sessa WC. Nitric oxide production contributes to the angiogenic properties of vascular endothelial growth factor in human endothelial cells. *J Clin Invest.* 1997;100: 3131–3139.
8. Ziche M, Morbidelli L, Masini E, Amerini S, Granger HJ, Maggi CA, Geppetti P, Ledda F. Nitric oxide mediates angiogenesis in vivo and endothelial cell growth and migration in vitro promoted by substance P. *J Clin Invest.* 1994;94:2036–2044.
9. Ziche M, Morbidelli L, Choudhuri R, Zhang HT, Donnini S, Granger HJ, Bicknell R. Nitric oxide synthase lies downstream from vascular endothelial growth factor–induced but not fibroblast growth factor–induced angiogenesis. *J Clin Invest.* 1997;99:2625–2634.

10. Murohara T, Asahara T, Silver M, Bauters C, Masuda H, Kalka C, Kearney M, Chen D, Symes JF, Fishman MC, Huang PL, Isner JM. Nitric oxide synthase modulates angiogenesis in response to tissue ischemia. *J Clin Invest.* 1998;101:2567–2578.
11. Amano K, Matsubara H, Iba O, Okigaki M, Fujiyama S, Imada T, Kojima H, Nozawa Y, Kawashima S, Yokoyama M, Iwasaka T. Enhancement of ischemia-induced angiogenesis by eNOS overexpression. *Hypertension.* 2003;41:156–162.
12. Arcangelo DD, Facchiano F, Barlucchi LM, Melillo G, Illi B, Testolin L, Gaetano C, Capogrossi MC. Acidosis inhibits endothelial cell apoptosis and function and induces basic fibroblast growth factor and vascular endothelial growth factor expression. *Circ Res.* 2000;86:312–318.
13. Iba O, Matsubara H, Nozawa Y, Fujiyama S, Amano K, Mori Y, Kojima H, Iwasaka T. Angiogenesis by implantation of peripheral blood mononuclear cells and platelets into ischemic limbs. *Circulation.* 2002;106:2019–2025.
14. Tateishi-Yuyama E, Matsubara H, Murohara T, Ikeda U, Shintani S, Masaki H, Amano K, Kishimoto Y, Yoshimoto K, Akashi H, Shimada K, Iwasaka T, Imaizumi T. Therapeutic angiogenesis for patients with limb ischemia by autologous transplantation of bone marrow cells: a pilot study and a randomised controlled trial. *Lancet.* 2002;360:427–435.
15. Fujiyama S, Amano K, Uehira K, Yoshida M, Nishiwaki Y, Nozawa Y, Jin D, Takai S, Miyazaki M, Egashira K, Imada T, Iwasaka T, Matsubara H. Bone marrow monocyte–lineage cells adhere on injured endothelium by MCP-1–dependent manner and accelerate reendothelialization as endothelial progenitor cells. *Circ Res.* 2003;93:980–989.
16. Peichev M, Naiyer AJ, Pereira D, Zhu Z, Lane WJ, Williams M, Oz MC, Hicklin DJ, Witte L, Moore MA, Rafii S. Expression of VEGF-2 and AC133 by circulating human CD34+ cells identified a population of functional endothelial precursors. *Blood.* 2000;95:952–958.
17. Kabrun N, Buhring HJ, Choi K, Ullrich A, Risau W, Keller G. Flk-1 expression defines a population of early embryonic hematopoietic precursors. *Development.* 1997;124:2039–2048.
18. Savin E, Balliart O, Bonnin P, Bedu M, Cheynel J, Coudert J, Martineaud JP. Vasomotor effects of transcutaneous CO_2 in stage II peripheral occlusive arterial disease. *Angiology.* 1995;46:785–791.
19. Hartmann BR, Bassenge E, Pittler M. Effect of carbon dioxide–enriched water and fresh water on the cutaneous microcirculation and oxygen tension in the skin of the foot. *Angiology.* 1997;48:337–343.
20. Toriyama T, Kumada Y, Matsubara T, Murata A, Ogino A, Hayashi H, Nakashima H, Takahashi H, Matsuo H, Kawahara H. Effect of artificial carbon dioxide foot bathing on critical limb ischemia (Fontaine IV) in peripheral arterial disease patients. *Int Angiol.* 2002;21:367–373.
21. Asahara T, Takahashi T, Masuda H, Kalka C, Chen D, Iwaguro H, Inai Y, Silver M, Isner JM. VEGF contributes to postnatal neovascularization by mobilizing bone marrow–derived endothelial progenitor cells. *EMBO J.* 1999;18:3964–3972.
22. Ku DD, Zaleski JK, Liu S, Brock TA. Vascular endothelial growth factor induces EDRF-dependent relaxation in coronary arteries. *Am J Physiol.* 1993;265:H586–H592.
23. van der Zee R, Murohara T, Luo Z, Zollmann F, Passeri J, Lekutat C, Isner JM. Vascular endothelial growth factor (VEGF)/vascular permeability factor (VPF) augments nitric oxide release from quiescent rabbit and human vascular endothelium. *Circulation.* 1997;95:1030–1037.
24. Bauters C, Asahara T, Zheng LP, Takeshita S, Bunting S, Ferrara N, Symes JF, Isner JM. Recovery of disturbed endothelium-dependent flow in the collateral-perfused rabbit ischemic hindlimb after administration of vascular endothelial growth factor. *Circulation.* 1995;91:2802–2809.
25. Aicher A, Heeschen C, Mildner-Rihm C, Urbich C, Ihling C, Technau-Ihling K, Zeiher AM, Dimmeler S. Essential role of endothelial nitric oxide synthase for mobilization of stem and progenitor cells. *Nat Med.* 2003;9:1370–1376.
26. Ferrara N, Alitalo K. Clinical application of angiogenic growth factors and their inhibitors. *Nat Med.* 1999;5:1359–1364.

Available online at www.sciencedirect.com
SCIENCE DIRECT®
Journal of Molecular and Cellular Cardiology 37 (2004) 775–784
Journal of Molecular and Cellular Cardiology
www.elsevier.com/locate/yjmcc

Original Article

Cytokine-induced nitric oxide inhibits mitochondrial energy production and induces myocardial dysfunction in endotoxin-treated rat hearts

Tetsuya Tatsumi [a,*,1], Kazuko Akashi [a,1], Natsuya Keira [a], Satoaki Matoba [a], Akiko Mano [a], Jun Shiraishi [a], Satoshi Yamanaka [a], Miyuki Kobara [a], Nobuhiro Hibino [b], Satoru Hosokawa [b], Jun Asayama [a], Shinji Fushiki [c], Henry Fliss [d], Masao Nakagawa [a], Hiroaki Matsubara [a]

[a] *Department of Cardiovascular Medicine, Kyoto Prefectural University of Medicine, Kawaramachi-Hirokoji, Kamigyo-ku, Kyoto 602 8566, Japan*
[b] *Drug Safety Research Laboratories, Eizai Co. Ltd, Takehaya, Kawashima Industrial Park, Kawashima-cho, Hashima, Gifu 501 6024, Japan*
[c] *Department of Dynamic Pathology, Kyoto Prefectural University of Medicine, Kawaramachi-Hirokoji, Kamigyo-ku, Kyoto 602 8566, Japan*
[d] *Department of Cellular and Molecular Medicine, University of Ottawa, 451 Smyth, Ottawa, Ont. K1H 8M5, Canada*

Received 9 April 2004; received in revised form 24 May 2004; accepted 18 June 2004

Abstract

The mechanism responsible for cardiac depression in septic shock remains unknown. The present study examined whether nitric oxide (NO) overproduced by inducible NO synthase (iNOS) can inhibit aerobic energy metabolism and impair the myocardial function in endotoxin-treated rat hearts. Lipopolysaccharide (LPS) significantly decreased systolic blood pressure (BP) to 44% of control during the 48 h treatment. Hearts from control and LPS-treated rats were perfused in a Langendorff apparatus. After LPS injection, left ventricular (LV) developed pressure (LVDP) was significantly depressed, plasma NO_2^-/NO_3^- (NO_x) concentration was markedly increased, and myocardial adenosine 5'-triphosphate (ATP), creatine phosphate (CrP), and the ratio of ATP/adenosine 5'-diphosphate were progressively decreased with time. Immunological examination showed a significant expression of iNOS protein in the LPS-treated myocytes. Aminoguanidine, an inhibitor of iNOS, significantly attenuated these LPS-induced functional and metabolic changes. Myocardial cyclic guanosine 3',5'-monophosphate (cGMP) content was significantly increased after LPS injection. Methylene blue, an inhibitor of soluble guanylate cyclase, blunted this increase in cGMP and significantly restored the LPS-induced contractile dysfunction 6 h after LPS injection. In addition, there was a significant negative correlation between LVDP and myocardial cGMP levels as well as a significant negative correlation between LVDP and plasma NO_x levels. In contrast, 48 h after LPS injection, methylene blue no longer affected cardiac performance, and there was a significant positive correlation between LVDP and myocardial ATP content. Furthermore, the normalized activities (as a ratio of the citrate synthase activity) of mitochondrial NADH-CoQ reductase, succinate-CoQ reductase, and ATPase, were significantly inhibited, and the swelling or disruption of mitochondria cristae was seen in the 48 h LPS treatment. These LPS-induced functional and morphological disorders in the mitochondria were significantly improved by aminoguanidine. The findings suggest that sustained production of NO by iNOS leads to contractile dysfunction via cGMP in the early stage, but that it can directly impair the mitochondrial function, lower myocardial energy production, and contribute significantly to the myocardial dysfunction in the later stage of septic shock.
© 2004 Elsevier Ltd. All rights reserved.

Keywords: Nitric oxide; Lipopolysaccharide; Cytokine; Endotoxin shock; Mitochondrial dysfunction

Abbréviations: ATP, adenosine 5'-triphosphate; ADP, adenosine 5'-diphosphate; AMP, adenosine 5'-monophosphate; CrP, creatine phosphate; CGMP, cyclic guanosine 3',5'-monophosphate; iNOS, inducible nitric oxide synthase; LPS, lipopolysaccharide; NO, nitric oxide; NO_x, NO_2^-/NO_3^-.

* Corresponding author. Tel.: +81-075-251-5511; fax: +81-075-251-5514.
E-mail address: tatsumi@koto.kpu-m.ac.jp (T. Tatsumi).

0022-2828/$ - see front matter © 2004 Elsevier Ltd. All rights reserved.
doi:10.1016/j.yjmcc.2004.06.014

1. Introduction

Septic shock is a major cause of morbidity and mortality in patients with septicemia [1], and is characterized by sustained hypotension, reduced responsiveness to vasoconstrictor agents, vascular damage, and hypoperfusion, resulting in multiple organ damage [2]. While cardiac output may be normal or elevated early in septic shock, recent clinical and experimental studies have shown that myocardial contractility is markedly impaired in the later stages of septic shock [3]. Although it is well documented that endotoxin-induced vascular collapse is mediated by nitric oxide (NO) [4,5], the mechanism responsible for cardiac depression in septic shock is still unknown. Studies performed in vitro, however, have reported that endotoxin-treated cardiac myocytes show depressed contractile function, which is attenuated by NO synthase (NOS) inhibitors [6,7], and that several cytokines, such as interleukin (IL)-2, IL-6, and tumor necrosis factor (TNF)-α produce a negative inotropic effect on isolated papillary muscle preparations through a NO-dependent mechanism [8]. Thus, in septic shock, it is expected that a number of pro-inflammatory cytokines are released locally or circulating levels of cytokines are elevated, and that NO-induced by endotoxin as well as cytokines mediates inhibition of myocardial contractility [9–11].

Although NO activates soluble guanylate cyclase to generate cyclic guanosine 3',5'-monophosphate (cGMP), a mediator capable of decreasing myocardial contractility [7,12–14], it is still largely uncertain how enhanced NO generation causes sustained reduction of myocardial contractility or myocardial damage. One of the interesting actions of NO is its inhibitory effect on aerobic energy production, since it is well known that sepsis is frequently characterized by a number of metabolic abnormalities, including increased plasma lactate concentrations and metabolic acidosis [15,16]. Previous studies have indicated that excessive amounts of NO produced by inducible NOS (iNOS) can cause deleterious disturbances in energy balance through the inhibition of mitochondrial respiration in a variety of cells [17,18]. In this regard, we have recently demonstrated that cytokine-induced NO production can lower myocardial energy production and induce contractile dysfunction in cultured rat cardiac myocytes [19]. These studies, however, have been conducted using isolated systems to examine the role of NO in contractile dysfunction, and it is still uncertain whether sustained NO production can affect myocardial energy metabolism and function in intact beating hearts.

In the present study, therefore, we tested our hypothesis that prolonged enhancement of NO production by iNOS can inhibit the endogenous aerobic energy producing pathways and depress myocardial function, independently of myocardial cGMP synthesis, in in vivo model of endotoxin-treated rat hearts. According to a previously established method [20], we used *Salmonella typhosa (S. typhosa)* lipopolysaccharide (LPS) to stimulate iNOS. We measured left ventricular (LV) developed pressure (LVDP) of the isolated perfused rat heart, and monitored plasma NO_2^-/NO_3^- (NO_x) concentrations as well as myocardial adenosine 5'-triphosphate (ATP), creatine phosphate (CrP), and ATP/adenosine 5'-diphosphate (ADP), to determine whether NO causes disruption of energy production. In addition, we measured the activities of mitochondrial iron sulfur enzymes, NADH-coenzyme Q (CoQ) reductase (complex I), succinate-CoQ reductase (complex II), oligomycin-sensitive ATPase (complex V), and citrate synthase, to determine the direct effects of NO on respiratory chain enzymes. Furthermore, we examined the iNOS expression and the mitochondrial ultrastructural disturbance in the endotoxin-treated hearts by immunohistochemical and electron microscopic examinations.

2. Materials and methods

2.1. Experimental protocol

All animals were handled in accordance with the *Guide for the Care and Use of Laboratory Animals*, US National Institute of Health (NIH publication No. 85–23, revised 1985). The protocol was approved by Bioethics Committe of the Kyoto Prefectural University of Medicine. Adult male Sprague–Dawley rats, weighing 250–320 g, were used in this experiment. Systolic blood pressure (BP) was monitored using tail cuffs, blood samples were taken, and plasma NO_x concentration was measured before, or 6, 24, and 48 h after *S typhosa* LPS (15 mg/kg body weight) was injected intravenously every 24 h. Rats were anesthetized with intraperitoneal sodium pentobarbital (60 mg/kg body weight) and heparin (1000 IU/kg body weight) was injected intravenously. Then the hearts were perfused in a Langendorff apparatus, and cardiac performance (LVDP) was evaluated 20 min after an equilibration period, and some of them were used for the assay of myocardial cGMP, adenine nucleotides, CrP, and creatine (Cr). To examine the role of iNOS in LPS-induced cardiac dysfunction, aminoguanidine (15 mg/kg body weight) was injected intraperitoneally 1 h before LPS injection. To examine the role of myocardial cGMP in LPS-induced cardiac dysfunction, methylene blue (10 mg/kg body weight) was injected intravenously 10 min before the hearts were excised. Forty-eight hours after LPS injection, immunological, and electron microscopic examinations were performed, and hearts were homogenized according to the indicated protocols for mitochondrial enzyme assay. Rats injected intravenously with saline alone were served as control.

2.2. Myocardial function

The procedure of perfusion for isolated hearts was described previously [21]. After rats were anesthetized with

[1] These two authors contributed equally to the work described in this manuscript.

sodium pentobarbital, the hearts were rapidly excised and placed in ice-cold saline. The connective tissue was removed rapidly, and the hearts were retrogradely perfused via the aorta at a constant perfusion pressure of 80 mmHg, with Krebs–Henseleit buffer consisting of 118 mmol/l NaCl, 4.7 mmol/l KCl, 1.2 mmol/l $MgSO_4$, 1.2 mmol/l KH_2PO_4, 1.8 mmol/l $CaCl_2$, 25 mmol/l $NaHCO_3$, and 11 mmol/l glucose, pH 7.4, oxygenated with 95% O_2 and 5% CO_2 at 37 °C. The atria were removed and the hearts were placed at 270 beats/min via two pacing wires inserted into the right ventricular myocardium. A water-filled latex balloon was inserted into the LV through the mitral valve for the measurement of LVDP. The LV end-diastolic pressure (LVEDP) was adjusted to 5–10 mmHg during the initial equilibration. LVDP was recorded continuously on a chart recorder (NEC, Tokyo, Japan).

2.3. NO_x assay

Plasma NO_x concentrations were determined with an autoanalyzer (ENO-10, Eicom Co., Kyoto, Japan). Samples were applied to an analytical column combined with a copperized cadmium reduction column to reduce NO_2^- to NO_3^-, which was then reacted with Griess reagent, to produce a product absorbing at 540 nm [22]. NO_2^- and NO_3^- were used as reference standards.

2.4. Myocardial adenine nucleotides, CrP, and Cr

Langendorff perfused hearts in control and LPS-treated hearts after 6, 24, and 48 h were freeze-clamped with Wollenberger tongs pre-chilled in liquid nitrogen after a stabilization period of 20 min. The hearts were kept in liquid nitrogen, and were then lyophilized overnight. Forty to sixty milligrams of lyophilized tissue was homogenized in 0.6 N ice-cold perchloric acid and was centrifuged at 2000 rpm for 10 min at 4 °C. The supernatants were neutralized with KOH to pH 5.0–7.0. After 10 min the extracts were centrifuged to remove $KClO_4$, and the supernatants were used for the assays. Cr, CrP, ATP, ADP, and adenosine 5'-monophosphate (AMP) contents were measured by high-performance liquid chromatography (HPLC: LC-9A liquid chromatograph, Shimadzu, Kyoto, Japan) with a column of STR ODS-M (Shimadzu) and were presented as μmol/g dry weight [21].

2.5. Myocardial cGMP content

cGMP concentration in the heart tissue was measured as follows. Langendorff perfused hearts were freeze-clamped with Wollenberger tongs pre-chilled in liquid nitrogen, and 200–300 mg of heart tissue was treated with 0.25 ml of ice-cold 6% trichloroacetic acid, and was centrifuged at 1000 *g* for 10 min. The supernatant was extracted three times with 3 ml of diethyl ether saturated with water, and the aqueous phase was stored at –80 °C. The cGMP concentration in the supernatant was measured by radioimmunoassay [23]. Briefly, a 0.1 ml of dioxane-triethylamine mixture containing succinic acid anhydride succinylated cGMP was added to the supernatant (0.1 ml). After 10 min incubation, the reaction mixture was added to 0.8 ml of 0.3 mol/l imidazole buffer (pH 6.5). Succinyl cGMP tyrosine methyl ester (0.1 ml) iodinated with ^{125}I (15 000–20 000 cpm in $<10^{-14}$ mol/l) was added to the assay mixture containing 0.1 ml of supernatant and 0.1 ml of diluted antisera and the mixture was incubated at 4 °C for 20 h. A cold solution of dextran-coated charcoal (0.5 ml) was added to the mixture in an ice-cold water bath. The charcoal was spun down, and 0.5 ml of the supernatant was counted for radioactivity in a gamma spectrometer. The amount of cGMP was normalized to the protein content of cardiac myocytes assayed by the Lowry's method [24].

2.6. Preparation of heart homogenates

At the end of the experimental protocol the heart was immediately immersed in ice-cold phosphate buffered saline (PBS). The ventricular myocardium was isolated, and was minced into very small pieces with scissors in 1.8 ml of a solution containing 50 mmol/l Tris–buffer (pH 7.5), 100 mmol/l KCl, 5 mmol/l $MgSO_4$, 1 mmol/l EGTA, and 0.5 mmol/l phenylmethanesulfonyl fluoride (PMSF). The minced heart tissue was homogenized with a Polytron PT 10–35 tissue processor (Kinematica Instrument) three times at a setting of seven for 10 sec, and the homogenate was centrifuged at 1000 *g* for 10 min [25]. The supernatant was stored at –80 °C until mitochondrial enzyme assay. The protein concentration in the supernatant was determined by the Lowry method [24].

2.7. Mitochondrial enzyme activity

Mitochondrial NADH-CoQ reductase activity was assayed spectrophotometrically at 37 °C by measuring the initial rate of NADH oxidation at 340 nm in the presence or absence of rotenone (15 mmol/l), according to the method of Hatefi and Rieske [26]. Briefly, aliquots of heart homogenates were added to 1 ml of a reaction buffer containing 10 mmol/l K_2HPO_4, 10 mmol/l KH_2PO_4, 2 mmol/l NaN_3, 0.35 mmol/l NADH, and 0.05 mmol/l CoQ1, pH 8.0.

Mitochondrial succinate-CoQ reductase activity was assayed spectrophotometrically at 37 °C by measuring the reduction of 2,6-dichloroindophenol sodium (DCIP) at 600 nm, according to the method of Ziegler and Rieske [27]. Aliquots of heart homogenates were added to 1 ml of a reaction buffer containing 50 mmol/l K_2HPO_4, 50 mmol/l KH_2PO_4, 0.0015% DCIP, 20 mmol/l sodium succinate, 0.01 mmol/l EDTA, 0.01% TritonX-100, and 0.05 mmol/l CoQ1, pH 7.0.

Mitochondrial ATPase activity was measured spectrophotometrically by coupling the reaction to a pyruvate kinase and lactate dehydrogenase system, according to the method of Lowe [28]. Briefly, aliquots of heart homogenates were added to 1 ml of a reaction buffer, containing 5 mmol/l

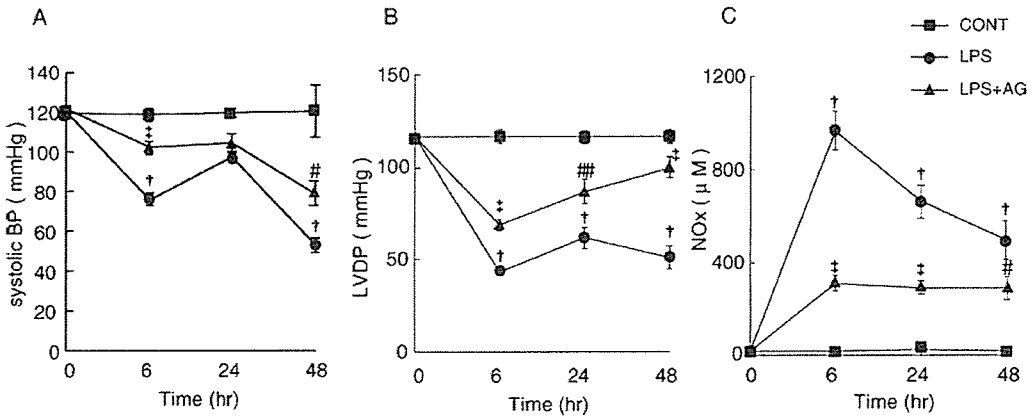

Fig. 1. Time course of changes in systolic BP, LVDP, plasma NO_x levels after saline (CONT) or LPS injection. Aminoguanidine (AG) was injected intraperitoneally 30 min before LPS treatment, and systolic BP (panel A), LVDP (panel B), and plasma NO_x concentration (panel C) were measured before (0 h), or at 6, 24, and 48 h after LPS injection, as described in Section 2. $^{\dagger}P < 0.001$ vs. CONT, $^{\#}P < 0.05$ vs. LPS, $^{\#\#}P < 0.01$ vs. LPS, $^{\ddagger}P < 0.001$ vs. LPS $n = 6$.

phosphoenol pyruvate, 50 mg pyruvate kinase, 50 mg lactate dehydrogenase, 25 mmol/l Tris–H_2SO_4, 5 mmol/l $MgSO_4$, 0.35 mmol/l NADH, and 2.5 mmol/l ATP, pH 8.0. Mitochondrial ATPase activity was determined at 37 °C by monitoring the decline of NADH oxidation at 340 nm in the presence or absence of oligomycin (10 ng/ml).

Citrate synthase was determined as described by Sheperd and Garland [29]. Briefly, aliquots of heart homogenates were added to 1 ml of a reaction buffer, containing 0.1 mol/l Tris–HCl; pH 8.0, 0.5 μmol/l oxaloacetate, 0.2 μmol/l 5,5'-dithiobis-(2-nitrobenzoic acid) (DTNB), 0.1 μmol/l acetyl-CoA, 0.1% TritonX. Citrate synthase activity was measured at 25 °C by chemical coupling of CoASH to DTNB at 412 nm.

2.8. Immunohistochemistry

The perfused rat hearts were embedded in OCT compound (Sakura Fine Technical Co. Ltd., Tokyo, Japan) and frozen in liquid nitrogen. Samples were stocked in −80 °C until cutting. Ten-micrometer sections were cut with a cryostat, air-dried for 2 h, and rinsed in PBS. For the inhibition of endogenous peroxidase activity, the specimens were incubated with methanol containing 1% H_2O_2 for 15 min. Then they were incubated with PBS containing 3% non-fat dry milk for 30 min and then incubated with blocking buffer (10% normal goat serum) for 10 min. Subsequently, the slides were incubated with mouse anti-iNOS antibody (Transduction Laboratories, Lexington, KY, USA) 1500 times diluted with PBS for 6 h at 4 °C. Then they were fixed with 4% paraformaldehyde for 10 min on ice. After washing in PBS, they were covered with biotinylated goat antiserum to mouse immunoglobulin G and a complex of streptavidin–biotin-conjugated with peroxidase for 30 min. Peroxidase activity was visualized with 0.25% diamino benzidine and 7.5×10^{-6}% H_2O_2 for 5 min at room temperature and counter stained with hematoxylin [30].

2.9. Electron microscopy

For electron microscopy, the perfused rat hearts were fixed in phosphate buffered 2.0% glutaraldehyde, postfixed in 1.0% osmium tetroxide, and embedded in epoxy resin. Ultrathin sections were stained with uranyl acetate and lead compound, and then examined with a JEM 100S electron microscope.

2.10. Statistical analysis

All experiments were repeated at least six times and the data are expressed as mean ± S.E. The data in Fig. 1 were analyzed by two-way analysis of variance (ANOVA), and the data in Figs. 3–5 were analyzed by one-way analysis of variance (ANOVA) and Bonferroni's multiple comparison. A P-value of less than 0.05 was considered statistically significant.

3. Results

3.1. Systolic BP, myocardial function, and plasma NO_x levels

The time course of changes in systolic BP, LVDP, and plasma NO_x concentration after LPS administration are illustrated in Fig. 1. Systolic BP was significantly decreased to 52.8 ± 3.6 mmHg, compared with control (120.3 ± 13 mmHg), 48 h after LPS injection. Aminoguanidine significantly attenuated the LPS-induced decline in systolic BP. LVDP was 113.6 ± 3.0 mmHg and coronary flow rate was 17 ± 2.3 ml/min in control hearts. Although the coronary flow rate did not significantly change (data not shown), LVDP was significantly depressed with time, reaching a minimum of 39% of control 6 h after LPS injection, and was slightly increased with time. Plasma NO_x level was 17.4 ± 1.5 μmol/l under control conditions. It was dramati-

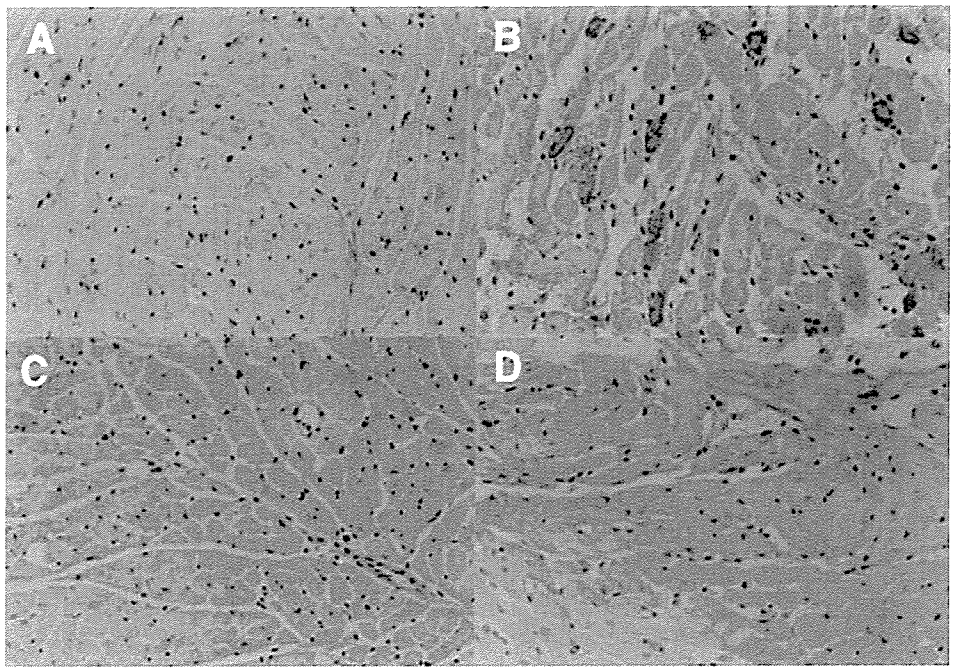

Fig. 2. Immunostaining for iNOS in LPS-treated hearts. The hearts isolated 48 h after saline (CONT) or LPS injection either in the presence or absence of aminoguanidine (AG) were perfused in a Langendorff apparatus, and iNOS protein was stained, as described in Section 2. (A) Control heart, (B) LPS-treated heart, (C) LPS-treated heart with AG, (D) LPS-treated heart omitting primary antibody (magnification ×200). The figure is representative of at least three similar experiments.

cally increased, reaching a maximum of 56 times the control levels 6 h after LPS injection, and was gradually decreased with time. Forty-eight hours after LPS injection, LVDP was decreased and plasma NO_x level was increased to 44% and 28 times the control levels, respectively. Aminoguanidine significantly attenuated the LPS-induced contractile dysfunction and increase in plasma NO_x levels.

3.2. iNOS expression

Fig. 2 illustrates immunohistochemical staining for iNOS protein in the hearts-treated with LPS for 48 h. Strong positive staining was seen mainly in the myocytes (Fig. 2B), although there was no immunoreactivity to iNOS protein in the control hearts (Fig. 2A). Cotreatment with aminoguani-

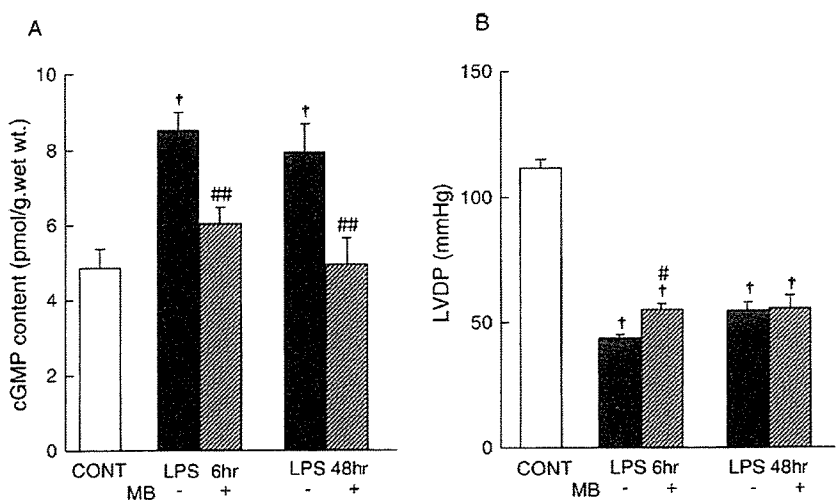

Fig. 3. Effect of methylene blue (MB) on (cGMP) content and LVDP. At 6 or 48 h after treatment with saline (CONT) or LPS, the hearts were perfused in a Langendorff apparatus. MB was injected intravenously 10 min before the hearts were excised, and myocardial cGMP content and LVDP were measured, as described in Section 2. $^{\dagger}P < 0.001$ vs. CONT, $^{\#}P < 0.05$ vs. LPS alone, $^{\#\#}P < 0.01$ vs. LPS alone.

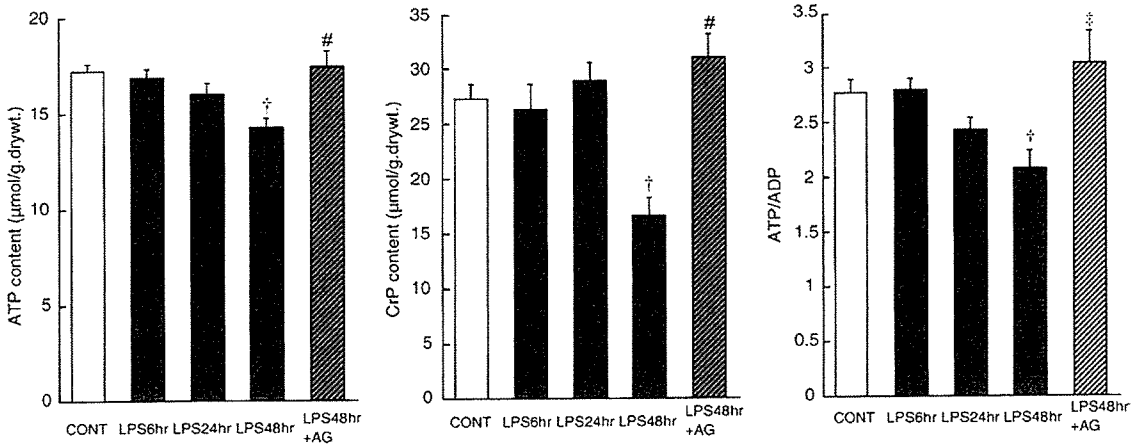

Fig. 4. Time course of changes in myocardial ATP, CrP, and ATP/ADP after LPS injection. Myocardial adenine nucleotides and CrP contents were measured 48 h after saline injection (CONT) or at 6, 24, and 48 h after LPS injection, as described in Section 2. Aminoguanidine (AG) was injected intraperitoneally 30 min before LPS treatment. $^{\dagger}P < 0.001$ vs. CONT, $^{\#}P < 0.05$ vs. LPS 48 h, $^{\ddagger}P < 0.001$ vs. LPS 48 h.

dine and LPS significantly inhibited this iNOS expression in the myocytes (Fig. 2C). No positive staining for iNOS was seen in the section used for negative control staining (Fig. 2D). A typical iNOS immunoblot was also obtained with myocardial extracts from hearts isolated 48 h after LPS injection (data not shown).

3.3. Myocardial cGMP content

Myocardial cGMP content and LVDP in the hearts 6 and 48 h after LPS injection are illustrated in Fig. 3. LPS significantly increased myocardial cGMP content to 1.8 and 1.6 times the control, 6 and 48 h after LPS injection, respectively, with a significant decline in LVDP. Methylene blue significantly inhibited this LPS-induced increase in cGMP and blunted the decline in LVDP 6 h after LPS injection. In contrast, methylene blue no longer blocked the LPS-induced contractile dysfunction 48 h after LPS injection, although it significantly inhibited the LPS-induced increase in cGMP.

3.4. Myocardial ATP, CrP, and the ratio of ATP/ADP

Fig. 4 shows the time course of changes in myocardial ATP, CrP, and the ratio of ATP/ADP after LPS administration. Myocardial ATP and CrP contents in the control hearts were 17.2 ± 0.5 and 27.4 ± 1.5 μmol/g dry weight, respectively. The ATP and CrP contents in the LPS-treated hearts significantly decreased with time, reaching 82% and 61% of control, respectively, 48 h after LPS administration. In contrast, the total adenine nucleotides did not significantly change during LPS treatment, although the AMP and Cr contents showed the converse changes to ATP and CrP, respectively, 48 h after LPS administration (data not shown). The ratio of ATP/ADP was also significantly decreased to

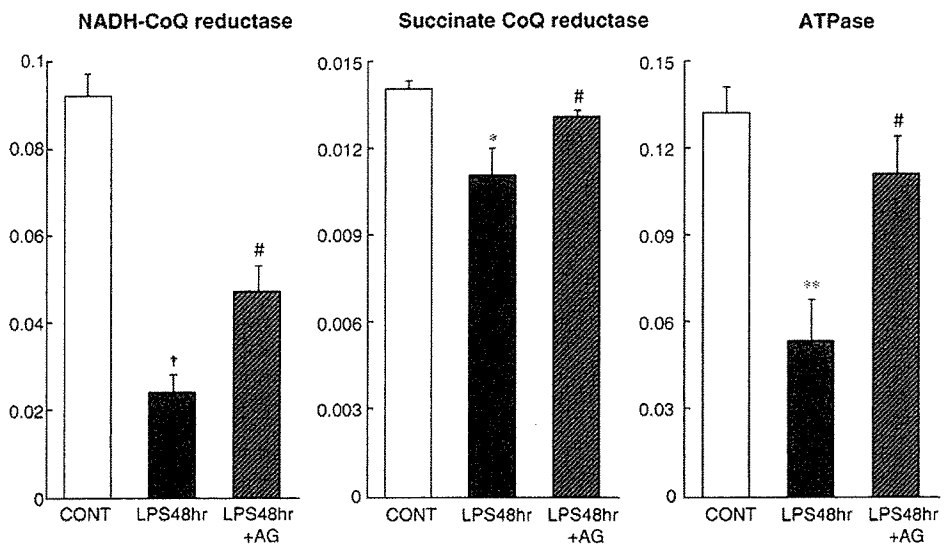

Fig. 5. Mitochondrial enzyme activities normalized as a ratio of citrate synthase activity in LPS-treated hearts. Rats were treated with saline (CONT) or LPS either in the presence or absence of aminoguanidine (AG) for 48 h. The activity of the indicated mitochondrial enzymes was assayed as described in Section 2. $^{*}P < 0.05$ vs. CONT, $^{**}P < 0.01$ vs. CONT, $^{\dagger}P < 0.001$ vs. CONT, $^{\#}P < 0.05$ vs. LPS alone.

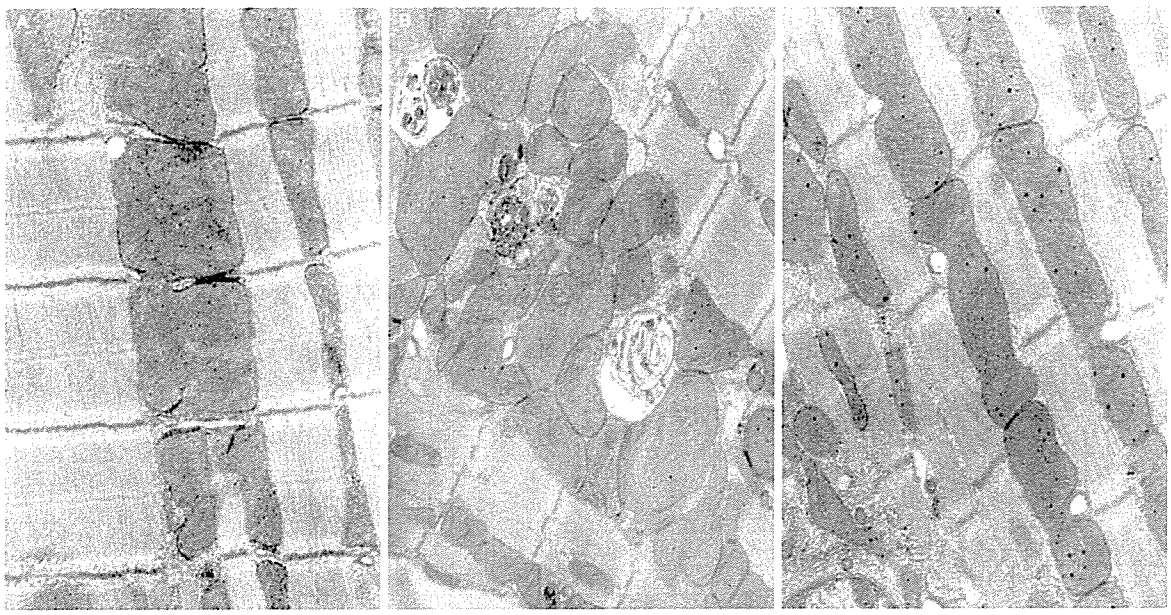

Fig. 6. Ultrastructure in LPS-treated hearts. The hearts isolated 48 h after saline (CONT) or LPS injection either in the presence or absence of aminoguanidine (AG) were perfused in a Langendorff apparatus, and mitochondrial morphology was examined by electron microscopy, as described in Section 2. (A) Control heart, (B) LPS-treated heart, (C) LPS-treated heart with AG. The figure is representative of at least three similar experiments.

75% of control 48 h after LPS administration. Aminoguanidine significantly attenuated these LPS-induced decline in myocardial ATP, CrP, and ATP/ADP.

3.5. Mitochondrial enzyme activities

Fig. 5 shows normalized activities (as a ratio of the activity of citrate synthase, a relatively stable mitochondrial marker enzyme) of NADH-CoQ reductase, succinate-CoQ reductase, and oligomycin-sensitive ATPase in the control and LPS-treated hearts for 48 h. The citrate synthase activity was not significantly affected by LPS treatment. In contrast, the activities of NADH-CoQ reductase, succinate-CoQ reductase, oligomycin-sensitive ATPase were significantly lowered to 26% ($P < 0.0001$), 79% ($P < 0.05$), and 40% ($P < 0.01$) of that in the control, respectively, 48 h after LPS injection. Aminoguanidine significantly blocked the LPS-induced depression of these enzyme activities.

3.6. Mitochondrial ultrastructure

Electron microscopic examination showed swelling of mitochondria or disruption of mitochondrial cristae in the hearts-treated with LPS for 48 h, as shown in Fig. 6. Cotreatment with aminoguanidine significantly inhibited the LPS-induced these ultrastructural changes.

3.7. Factors associated with myocardial function

The role of myocardial ATP content, plasma NO_x levels, myocardial cGMP content in cardiac contractile force was evaluated 6 and 48 h after LPS injection, as illustrated in Figs. 7 and 8, respectively. Six hours after LPS injection,

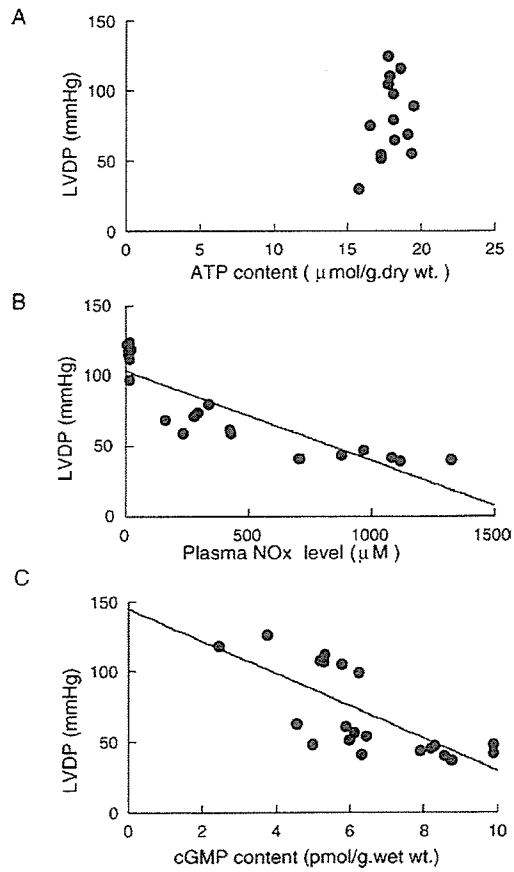

Fig. 7. Scatterplot showing the relation between LVDP and myocardial ATP content, plasma NO_x levels or myocardial cGMP content before or at 6 h after LPS injection. (A) There was no significant correlation. (B) The relation was $y = 103.6 - 0.064x$, $r = 0.864$, $P < 0.0001$, $n = 21$. (C) The relation was $y = 144.4 - 11.5x$; $r = 0.722$; $P < 0.005$; $n = 21$.

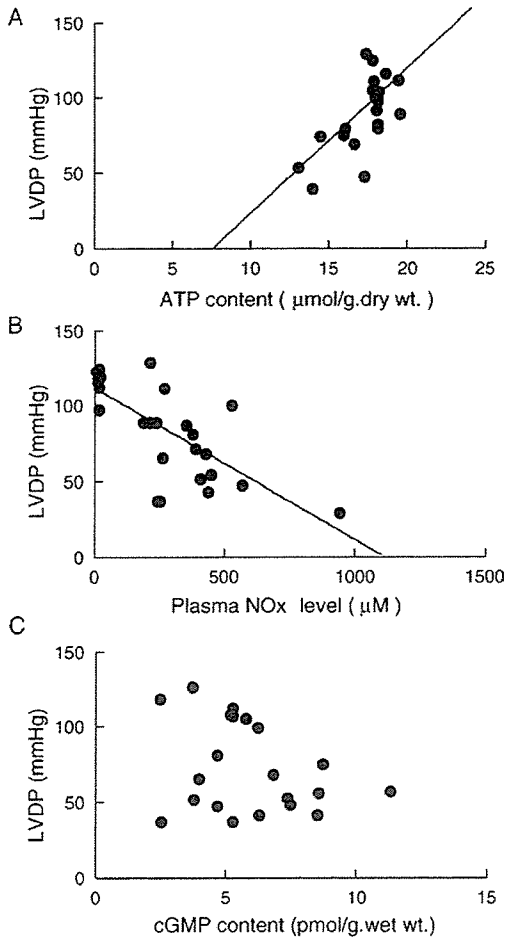

Fig. 8. Scatterplot showing the relation between LVDP and myocardial ATP content, plasma NO_x levels or myocardial cGMP content before or at 48 h after LPS injection. (A) The relation was $y = 75.8 + 9.62x$; $r = 0.674$; $P < 0.001$; $n = 21$. (B) The relation was $y = 120 - 0.101x$; $r = 0.718$; $P < 0.0001$; $n = 21$. (C) There was no significant correlation.

myocardial ATP content did not correlate with LVDP; however, there was a statistically significant negative correlation between LVDP and either plasma NO_x concentration ($r = 0.864$, $P < 0.0001$) or myocardial cGMP content ($r = 0.722$, $P < 0.005$) (Fig. 7). In contrast, 48 h after LPS injection, there was a statistically significant positive correlation between LVDP and ATP content ($r = 0.674$, $P < 0.001$) as well as a statistically significant negative correlation between LVDP and NO_x concentration ($r = 0.718$, $P < 0.0001$), although there was no statistically significant correlation between LVDP and cGMP content (Fig. 8).

4. Discussion

It is presently well known that LPS as well as pro-inflammatory cytokines can upregulate the activity of iNOS in cardiac myocytes and produces a large amount of NO production [7,14,31,32]. Despite the fact that plasma levels of various cytokines are elevated [2,33], little is known about the mechanisms underlying the injurious effects of NO on the heart in endotoxemia. In this study, we have demonstrated for the first time that while excessively produced NO may induce myocardial dysfunction based on an increase in myocardial cGMP synthesis in the early stage, it can directly contribute to contractile dysfunction through the disturbance of mitochondrial respiratory activity and resultant myocardial energy depletion in the later stage of septic shock.

There have been only few studies examining the functional role of NO in endotoxin-induced contractile dysfunction, and those results using intact beating hearts are still controversial [3,20,34–36]. In the present study, the plasma NO_x concentration was markedly increased and LVDP was significantly depressed after LPS injection. We also confirmed significant expression of iNOS protein in the myocytes 48 h after LPS administration. In addition, the plasma concentrations of TNF-α and INF-γ, capable of expressing iNOS [18,34], were significantly increased after LPS administration (data not shown). These findings suggest that either the cytokines produced by LPS or LPS directly induced iNOS expression. Cotreatment of rats with aminoguanidine and LPS inhibited myocardial iNOS expression, reduced plasma NO_x concentration, and significantly improved the LPS-induced cardiac dysfunction, strongly suggesting that NO produced by iNOS mediates these functional and metabolic changes in endotoxin-treated rats.

One of the important potential mechanisms of contractile dysfunction in endotoxemia is the NO–cGMP pathway, because in vitro studies have reported that cGMP is a mediator capable of decreasing myocardial cytoplasmic Ca^{2+} concentration [7,12–14]. In this study, myocardial cGMP content was significantly increased after LPS injection. Methylene blue, an inhibitor of soluble guanylate cyclase, blunted this increase in cGMP content, and it significantly restored the LPS-induced contractile dysfunction 6 h after LPS injection. In addition, we confirmed that methylene blue did not affect plasma NO_x levels (data not shown). Furthermore, there was a significant negative correlation between LVDP and myocardial cGMP levels 6 h after LPS injection. In contrast, 48 h after LPS injection, methylene blue no longer affected cardiac performance, and there was no significant correlation between LVDP and myocardial cGMP. These results indicate that cGMP generated by NO significantly contributes to the LPS-induced cardiac dysfunction at least in the early stage, and suggest that some other factors regulate myocardial contractility in the later stage of septic shock.

Sepsis is frequently characterized by a number of metabolic abnormalities including increased plasma lactate concentration, metabolic acidosis, and enhanced glycolysis [15,16,37], which suggests that serious bioenergetic failure occurs in septic shock. However, the effect of sepsis on aerobic energy metabolism in various organs remains controversial. Several studies have reported that there were no significant differences in the levels of the Krebs cycle metabolites or high energy phosphates between the control and septic hearts [37–39]. In contrast, recent other studies dem-